

F. İslamoğlu* , N. Erdoğan , E. Hacıfazlıoğlu 

Recep Tayyip Erdoğan University, Rize, Turkey

*e-mail: fatih.islamoglu@erdogan.edu.tr

(Received October 19 2023; received in revised form November 13 2023; accepted November 28 2023)

Theoretical determination of electronic, geometric and spectroscopic properties of some 1,2,4-triazol derivatives

Abstract. In this study, molecular geometric optimization of five 4,5-dihydro-1H-1,2,4-triazol-5-one derivative compounds was obtained using Density Functional Theory, (DFT, B3LYP)/ Hartree Fock, (HF, B3LYP) methods on the basis set of 6-311G (d,p) in order to find the most stable geometric shape of the studied compounds. FT-IR and UV-vis spectral values were performed by using gauge independent atomic orbital (GIAO) methods with Gaussian G09W package program. IR frequency datas of investigated five compounds were calculated in gas phases and are multiplied with appropriate scala factors. The identification of the calculated IR data was performed in the veda4f program. In addition, bond angles, bond lengths, dipole moments, highest occupied molecular orbital (HOMO), lowest unoccupied molecular orbital (LUMO) energy and total energy, mulliken charges and molecular electrostatic potential (MEP) of five compounds were calculated using same methods and set.

Key words: Density functional theory, hartree fock, triazole derivatives.

Introduction

One of the most significant families of heterocyclic molecules includes triazoles and their derivatives. Due to their wide range of biological activities, 1,2,4-triazole derivatives have received a lot of attention in medicinal chemistry. Examples of these biological activities include antiviral [1], antibacterial [2], antifungal [3, 4] (examples of antifungal drugs are fluconazole [5, 6], itraconazole [7], ravuconazole [8], voriconazole [9-11] and posaconazole [12]), anti-tubercular [13-15], immunosuppressant [16], antihypertensive [17], anti-inflammatory [18,19], anticonvulsant [20, 21], analgesic [22], hypoglycemic [23], antidepressant [24, 25] and anticancer [26-28] activities. Derivatives of 1,2,4-triazoles are a significant class of antifungal medications that are frequently used to treat fungi [29]. Insecticides [30], antiasthmatics [31], antidepressants [32], insecticidal [33], and plant growth regulators [34] are all described uses for 1,2,4-triazole derivatives. Moreover, triazole-containing substances with anti-aromatase properties as vorozole, letrozole, and anastrozole have been demonstrated to be particularly helpful in preventing breast cancer [35-37]. According to reports, the 1,2,4-triazole moiety interacts well with heme iron, and the triazole's aromatic substituents

are particularly successful in interacting with the active site of aromatase [38, 39].

Several properties in chemical systems have been predicted using computational chemical simulations. Because of this, the design of functional materials has been heavily utilized in these computations. Several organic compounds' spectroscopic, electrical, and thermodynamic properties have been clarified utilizing theoretical calculation techniques [40-44]. Due to their strong biological activity, Mannich bases have been able to capture the interest of numerous researchers. Due to this, publications on Mannich bases and their derivatives computational chemical computations were reported in the literature [45-48]. In order to determine the structural, spectroscopic, and electrical properties of the title chemical, we used a theoretical analysis approach. First off, the B3LYP(DFT)/6-311G(d,p) and B3LYP(HF)/6-311G(d,p) basis set have been used for all quantum chemical calculations of the molecules in issue. The optimized structure with B3LYP/6-311G(d,p) level was used to determine the 1H and 13C-NMR chemical shift values, vibrational frequencies, structural, and electronic parameters, HOMO-LUMO energies, and molecular electrostatic potential maps (MEP) of the title molecule. The spectral information generated using DFT/B3LYP and the 6-311G(d,p) basis set was connected to the vibrational frequencies of the

named molecular structure. The calculated and taken from the literature of experimental values of every spectroscopic parameter were compared.

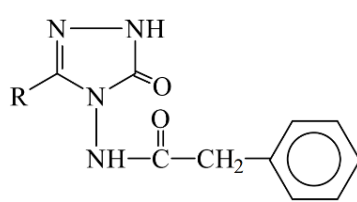
If the predicted frequencies are scaled to account for the approximation handling of electron correlation, for basis set shortcomings, and for the anharmonicity, density functional theory calculations (DFT) are said to provide excellent vibrational frequencies of organic compounds [49, 50]. Several publications in the literature have discussed the calculation of the chemical shift of the Nuclear Magnetic Resonance using quantum-chemistry techniques [51–55]. However, it was suggested that the single-point calculation of magnetic shielding by DFT methods was combined with a quick and accurate geometry-optimization procedure at the molecular mechanics level because as molecular size increases, computing-time limitations are introduced for obtaining optimized geometries at the DFT level [51].

One of the most popular methods for estimating nuclear magnetic shielding tensors is the gauge-including atomic orbital [56–57]. It has been demonstrated that, for the same basis set size, the results generated by the GIAO method are frequently

more accurate than those estimated using other approaches [58]. When the electron correlation contributions were not insignificant, DFT approaches were favoured for the analysis of large organic compounds [59] and for GIAO ¹³C calculations [58].

Materials and methods

Studied molecules. In this article, five 1,2,4-triazol derivatives ((1) N-(3-methyl-5-oxo-1,5-dihydro-4H-1,2,4-triazol-4-yl)-2-phenylacetamide, (2) N-(3-ethyl-5-oxo-1,5-dihydro-4H-1,2,4-triazol-4-yl)-2-phenylacetamide, (3) N-(3-benzyl-5-oxo-1,5-dihydro-4H-1,2,4-triazol-4-yl)-2-phenylacetamide, (4) N-{3-[(4-methylphenyl)methyl]-5-oxo-1,5-dihydro-4H-1,2,4-triazol-4-yl}-2-phenyl acetamide, (5) N-{3-[(4-chlorophenyl)methyl]-5-oxo-1,5-dihydro-4H-1,2,4-triazol-4-yl}-2-phenylacetamide) has been theoretically studied. Experimental studies on these molecules have been previously conducted and published as articles [60]. First of all, all molecules were optimized according to Density Functional Theory (DFT) and Hartree–Fock (HF) methods. Structure of the studied molecules is given on Figure 1.



	R
1	-CH ₃
2	-CH ₂ CH ₃
3	-CH ₂ C ₆ H ₅
4	-CH ₂ C ₆ H ₄ CH ₃ (<i>p</i> -)
5	-CH ₂ C ₆ H ₄ Cl (<i>p</i> -)

Figure 1 – Structure of the optimized molecules

Three dimensional drawing of molecules. The Gauss-view program is an interface included in the gaussian package programs that allows the three-dimensional design of a molecule to visually define the properties of the molecule, modify it, and start calculations by creating input data. Gaussview allows us to visualize molecules and move them in the direction we want, make changes in molecules and examine the results calculated for a molecule studied in the Gaussian 09W program. Gauss-view graphical interface program is used to facilitate the Gaussian 09W program according to the bond numbers and positions of the atoms in the molecule. With the Gauss-view program, formula groups, symbols of atoms and their bonding shapes are

available, and a three-dimensional Gauss-view image is obtained by using formulas and symbols and bonds that are suitable for the molecule to be drawn.

Bond angle and bond length. When determining and fine-tuning the structures of numerous molecules, correct knowledge of conventional bond lengths and bond angles is crucial. The experimental data from either X-ray crystallography or NMR studies are supplemented with ideal or target values for these geometrical parameters, which effectively increases the number of experimental observations in relation to the number of parameters being determined (the latter being the atomic co-ordinates and temperature factors). For the computational values of bond angle

and bond length, which are the geometrical structure parameters of all molecules, calculations were made using HF/DFT(B3LYP) methods and 6-311G(d,p) basic set in the Gaussian 09W package program.

Mulliken atomic charge. The electronic charge distribution in a molecule and the bonding, antibonding, or nonbonding nature of the molecular orbitals for specific atomic pairs can be described using Mulliken atomic charges. The concept of these Mulliken atomic charges was established; it was thought to be a real, normalized molecular orbital made up of two normalized atomic orbitals. The square of the wavefunction can be used to represent the charge distribution as a probability density. The result is obtained by integrating over all of the electronic coordinates and using the normalized molecular and atomic orbitals.

HOMO-LUMO. For the investigation of trends in -electronic configurations for conjugated systems simulated by different classes of chemical graphs, the HOMO-LUMO map has been proposed as a qualitative tool. The goal is to create a scatterplot of the Hückel HOMO vs LUMO eigenvalues and look at how the data clusters. The mappings proposed a conjecture for more general chemical graphs and a theorem for eigenvalue bounds for chemical trees. We used this simple device to re-examine some aspects of the qualitative theory of the electronic structure of 1,2,4-triazole derivatives and identify some plausible conjectures.

Dipole moment and total energy properties. When there is a separation of charge, dipole moments happen. Dipole moments, which result from variations in electronegativity, can happen between atoms in a covalent link or between two ions in an ionic bond. The dipole moment increases with the difference in electronegativity. The size of the dipole moment is also affected by the distance between the charge separations. The polarity of the molecule is determined by the dipole moment. By calculating the lowest feasible calculated energy, we may use the variation theorem to forecast the total energies of atoms. We can answer for the total energies of atoms with great precision using the outcomes of variation calculations, perturbation theory, Density Functional Theory, Hartree-Fock calculations, and/or configuration interaction.

IR spectral analysis. The study of how a molecule interacts with infrared light is known as infrared spectroscopy. Absorption, emission, and reflection measurements can be used to examine this in three

different ways. This method is mostly employed in organic and inorganic chemistry. Chemists employ it to identify functional groups in compounds. By measuring atom vibrations using IR spectroscopy, the functional groups of molecules can be identified. Usually, heavier atoms and stronger bonds will vibrate with a higher stretching frequency (wavenumber).

UV Spectral analysis. UV-visible spectroscopy is a technique used to analyze the electronic transitions of molecules in the ultraviolet (UV) and visible (VIS) regions of the electromagnetic spectrum. It involves passing a beam of light of a specific wavelength through a sample and measuring the intensity of the light that is transmitted or absorbed. In UV-visible spectroscopy, the energy of the light is absorbed by the molecule and causes an electronic transition from the ground state to an excited state. The energy required to cause this transition is dependent on the chemical structure of the molecule, and thus each molecule has a unique absorption spectrum.

Molecular electrostatic potential (MEP). Molecular electrostatic potential (MEP) is a measure of the electrostatic potential energy at a given point in space around a molecule. It is a tool used in computational chemistry to study the distribution of electric charge in a molecule and its relationship to the molecule's properties. MEP is calculated by solving the Schrödinger equation for the molecule using quantum mechanical methods. This provides a description of the electron density around the molecule, which in turn allows the calculation of the electrostatic potential at each point in space. MEP for studied molecules using IQmol computer program for 6-311G(d) level.

Results and discussion

First, the bond lengths and bond angles of the molecules given in Table 1-2 were examined. When we evaluate the bonds between molecules, the longest bond length is 1.75963 Å between C(38)-Cl(39) atoms in the 5th molecule according to the DFT model, and the shortest bond length is 0.99039 Å between N(1)-H(7) atoms in the 2nd molecule according to the HF model was determined. When we consider in terms of angles, the widest bond angle is 131.59799 degrees between N(1)-C(2)=O(5) atoms in the 3rd molecule according to the DFT model and the narrowest bond angle is 100.75592 degrees between N(1)-C(2)-N(4) atoms in the 4th molecule according to the DFT model was determined.

Table 1 – The calculated bond angles (θ) of all molecules as DFT (B3LYP) and HF (B3LYP) methods on the basis set of 6-311G (d,p).

Bond Angles ($^{\circ}$)	Molecule 1	Molecule 2	Molecule 3	Molecule 4	Molecule 5
	DFT / HF				
H(7)-N(1)-C(2)	125.51734 / 125.76726	125.51958 / 125.78813	125.56632 / 125.83578	125.54830 / 125.82899	125.56176 / 125.84750
N(1)-C(2)=O(5)	131.54741 / 131.18307	131.50846 / 131.15371	131.59799 / 131.20935	131.56212 / 131.20538	131.57251 / 131.21932
N(1)-C(2)-N(4)	100.79764 / 101.64543	100.79403 / 101.65701	100.76333 / 101.62205	100.75592 / 101.62204	100.76218 / 101.62323
C(2)-N(4)-C(25)	109.00053 / 108.58199	109.04967 / 108.64197	108.97677 / 108.56856	108.98419 / 108.58452	108.91670 / 108.52508
N(4)-C(25)=N(3)	110.75049 / 110.72141	110.63013 / 110.56702	110.72754 / 110.63954	110.71453 / 110.61622	110.81169 / 110.71254
C(25)=N(3)-N(1)	105.05126 / 105.44952	105.14484 / 105.55789	105.06021 / 105.50403	105.05873 / 105.50629	105.04301 / 105.49273
N(3)-N(1)-H(7)	120.08212 / 120.62360	120.10128 / 120.62720	119.95986 / 120.49493	119.96302 / 120.49679	119.96822 / 120.50083
N(3)=C(25)-C(26)	125.36200 / 125.77546	125.91522 / 126.48111	126.58605 / 127.22220	126.64688 / 127.25754	126.43192 / 127.05017
H(28)-C(26)-H(27)	109.19119 / 109.55612	113.17004 / 113.14622	105.52697 / 105.82943	105.47604 / 108.02927	105.51012 / 105.83383
H(27)-C(26)-H(29)	107.50943 / 107.88766	-	110.26828 / 110.37114	-	110.27807 / 110.37329
H(28)-C(26)-H(29)	109.14532 / 109.51700	105.39778 / 105.89996	-	-	-
N(4)-C(25)-C(26)	123.88734 / 123.88734	123.45458 / 122.95187	122.68550 / 122.13827	122.63660 / 122.12624	122.75449 / 122.23729
C(25)-N(4)-N(6)	126.25664 / 125.93893	126.26731 / 125.89747	-	-	-
N(4)-N(6)-H(8)	115.48168 / 114.73649	115.63506 / 114.77904	115.46198 / 114.70483	115.54557 / 114.72428	115.41126 / 114.62772
N(4)-N(6)-C(9)	123.96491 / 121.76834	124.15527 / 121.81280	123.93710 / 121.71803	124.04090 / 121.73215	123.92439 / 121.66206
N(6)-C(9)=O(10)	118.34852 / 118.40623	118.36627 / 118.43522	118.35174 / 118.41488	118.36853 / 118.43318	118.26233 / 118.34988
N(6)-C(9)-C(11)	117.53223 / 116.57779	117.56948 / 116.58107	117.54833 / 116.59035	117.54943 / 116.58199	117.57960 / 116.61053
C(9)-C(11)-H(24)	111.18608 / 106.24476	111.19498 / 109.38708	111.19580 / 106.24680	111.16192 / 106.24229	111.14887 / 106.26400
C(9)-C(11)-H(23)	105.88265 / 109.37203	105.94016 / 106.22629	105.88335 / 109.38740	-	-
H(23)-C(11)-H(24)	106.92516 / 106.52050	106.97496 / 106.52562	106.96904 / 106.52356	107.00132 / 106.51549	107.00100 / 106.51418
C(9)-C(11)-C(12)	112.20308 / 113.59009	112.07661 / 113.58893	112.14749 / 113.55114	112.10077 / 113.55415	112.10718 / 113.54258
H(8)-N(6)-C(9)	113.09749 / 112.87271	113.25459 / 112.92184	113.02707 / 112.77322	113.12165 / 112.79664	112.92556 / 112.67060
O(10)=C(9)-C(11)	123.99698 / 125.00887	123.95400 / 124.97705	123.97874 / 124.98744	123.96900 / 124.97758	124.04234 / 125.03183
C(11)-C(12)-C(15)	120.11333 / 120.70956	120.12823 / 120.71591	120.14590 / 120.68941	120.11513 / 120.69286	120.09381 / 120.67225

Table continuation

Bond Angles ($^{\circ}$)	Molecule 1	Molecule 2	Molecule 3	Molecule 4	Molecule 5
	DFT / HF				
C(11)-C(12)=C(17)	120.80145 / 120.46534	120.77136 / 120.46538	120.76011 / 120.48532	120.78723 / 120.48497	120.79365 / 120.49098
C(12)=C(17)-H(18)	119.58325 / 119.83456	119.57365 / 119.82820	119.57931 / 119.83749	119.57924 / 119.83444	119.60227 / 119.84954
H(24)-C(11)-C(12)	110.54616 / 110.49546	110.53736 / 110.49673	110.58156 / 110.50076	-	-
H(23)-C(11)-C(12)	109.85444 / 110.30918	109.88551 / 110.30744	109.82257 / 110.33337	109.85053 / 110.33409	109.84945 / 110.33356
C(12)=C(17)-C(16)	120.60550 / 120.76477	120.59195 / 120.76722	120.60424 / 120.76423	120.60457 / 120.76528	120.59117 / 120.75984
H(18)-C(17)-C(16)	119.81094 / 119.40046	119.83390 / 119.40439	119.81595 / 119.39815	119.81568 / 119.40015	119.80612 / 119.39049
C(17)-C(16)-H(19)	119.79467 / 119.78686	119.80222 / 119.78767	119.79459 / 119.79045	119.79564 / 119.78925	119.79472 / 119.79559
C(17)-C(16)=C(14)	120.05223 / 120.01650	120.05740 / 120.01731	120.05320 / 120.01637	120.05028 / 120.01759	120.05144 / 120.01212
C(16)=C(14)-H(22)	120.16083 / 120.23147	120.15890 / 120.23153	120.16367 / 120.22769	120.16269 / 120.22870	120.15672 / 120.22350
C(16)=C(14)-C(13)	119.66092 / 119.59057	119.66794 / 119.58860	119.65816 / 119.59138	119.65906 / 119.58987	119.66635 / 119.59777
C(14)-C(13)-H(21)	120.07682 / 120.04432	120.08252 / 120.04445	120.07632 / 120.04688	120.07179 / 120.04733	120.07575 / 120.04795
C(14)-C(13)=C(15)	120.28382 / 120.23409	120.27021 / 120.23505	120.28915 / 120.23103	120.29138 / 120.23142	120.28386 / 120.22914
C(13)=C(15)-H(20)	119.99873 / 119.74436	120.03393 / 119.74545	120.01165 / 119.74448	120.03926 / 119.74505	120.03707 / 119.74100
C(13)=C(15)-C(12)	120.31199 / 120.57274	120.31359 / 120.57503	120.30215 / 120.57479	120.29815 / 120.57678	120.29541 / 120.56723
H(21)-C(13)=C(15)	119.63924 / 119.72155	119.64710 / 119.72046	119.63440 / 119.72206	119.63673 / 119.72122	119.64029 / 119.72289
H(20)-C(15)-C(12)	119.68116 / 119.68153	119.64306 / 119.67814	119.67815 / 119.67945	119.65407 / 119.67689	119.65470 / 119.69054
H(7)-N(19)-C(2)	-	125.51958 / 125.78813	-	-	-
O(5)=C(2)-N(4)	-	127.68717 / 127.18339	127.62943 / 127.16283	126.67271 / 127.16680	127.65619 / 127.15181
C(2)-N(4)-N(6)	-	124.49850 / 124.96083	124.46635 / 124.96216	124.49208 / 124.93516	124.58774 / 125.03049
N(6)-N(4)-C(25)	-	126.25500 / 126.02905	126.33461 / 126.08436	126.29247 / 126.09151	126.25211 / 126.04678
C(25)-C(26)-H(28)	-	108.44966 / 108.19824	108.32520 / 107.90863	108.27469 / 107.85894	108.40364 / 108.02759
C(25)-C(26)-H(29)	-	108.45512 / 108.02851	113.79864 / 113.89156	-	-
C(26)-C(27)-H(31)	-	111.12290 / 111.15854	-	-	-
H(31)-C(27)-H(30)	-	108.49036 / 108.51343	-	-	-

Table continuation

Bond Angles ($^{\circ}$)	Molecule 1	Molecule 2	Molecule 3	Molecule 4	Molecule 5
	DFT / HF	DFT / HF	DFT / HF	DFT / HF	DFT / HF
H(31)-C(27)-H(32)	-	107.57557 / 107.86320	-	-	-
H(29)-C(26)-C(27)	-	110.53421 / 110.64248	-	-	-
C(26)-C(27)-H(30)	-	109.94303 / 109.59954	-	-	-
C(26)-C(27)-H(32)	-	111.12634 / 111.11717	-	-	-
H(32)-C(27)-H(30)	-	108.48694 / 108.50503	-	-	-
C(13)-C(14)-H(22)	-	120.17290 / 120.17985	120.17795 / 120.18091	120.17804 / 120.18142	120.17671 / 120.17871
C(14)=C(16)-H(19)	-	120.14034 / 120.19491	120.15215 / 120.19309	120.15401 / 120.19307	120.15378 / 120.19219
C(17)=C(12)-C(15)	-	119.09577 / 118.81677	119.09033 / 118.82218	119.09401 / 118.81904	119.10927 / 118.83387
C(25)-C(26)-H(27)	-	-	108.27295 / 108.08503	-	-
H(28)-C(26)-C(29)	-	-	110.28981 / 110.39942	-	-
C(26)-C(29)-C(31)	-	-	120.57816 / 120.57232	120.86662 / 120.86084	120.74635 / 120.71445
C(26)-C(29)-C(30)	-	-	120.57162 / 120.53591	120.81562 / 120.85875	120.66345 / 120.66706
C(29)-C(31)-H(35)	-	-	119.61982 / 119.79019	119.66057 / 119.82719	119.82376 / 119.95904
C(29)-C(31)-C(34)	-	-	120.65440 / 120.64907	120.80140 / 120.85120	121.10752 / 121.06711
C(32)-C(30)-C(29)	-	-	120.66281 / 120.63927	120.81521 / 120.85249	121.12816 / 121.06035
H(33)-C(30)-C(29)	-	-	119.62982 / 119.77614	119.69431 / 119.84109	119.82199 / 119.94732
C(30)-C(29)-C(31)	-	-	118.85021 / 118.89041	118.31751 / 118.27806	118.58995 / 118.61800
C(31)-C(34)-H(38)	-	-	119.80029 / 119.78413	-	-
C(31)-C(34)-C(36)	-	-	120.09126 / 120.09425	-	-
H(38)-C(34)-C(36)	-	-	120.10834 / 120.12154	-	-
C(34)-C(36)-H(39)	-	-	120.16716 / 120.18540	-	-
C(34)-C(36)-C(32)	-	-	119.66277 / 119.62450	-	-
H(39)-C(36)-C(32)	-	-	120.16990 / 120.18997	-	-
C(36)-C(32)-H(37)	-	-	120.12235 / 120.12140	-	-

Table continuation

Bond Angles ($^{\circ}$)	Molecule 1	Molecule 2	Molecule 3	Molecule 4	Molecule 5
	DFT / HF	DFT / HF	DFT / HF	DFT / HF	DFT / HF
C(36)-C(32)-C(30)	-	-	120.07852 / 120.10249	-	-
H(37)-C(32)-C(30)	-	-	119.79896 / 119.77602	-	-
C(32)-C(30)-H(33)	-	-	119.70736 / 119.58459	119.48996 / 119.30624	119.04984 / 118.99232
N(3)-N(1)-C(2)	-	-	-	114.47587 / 113.62284	114.45412 / 113.61732
H(27)-C(26)-C(29)	-	-	-	110.31199 / 110.40916	-
C(29)-C(26)-C(25)	-	-	-	113.92022 / 113.98235	113.62045 / 113.67489
H(35)-C(31)-C(34)	-	-	-	119.53796 / 119.32150	119.06866 / 118.97381
C(31)-C(34)-H(37)	-	-	-	119.40433 / 119.29469	120.78718 / 120.67751
H(37)-C(34)-C(38)	-	-	-	119.48461 / 119.63939	120.14655 / 120.16543
C(31)-C(34)-C(38)	-	-	-	121.11073 / 121.06563	119.06622 / 119.15702
C(34)-C(38)-C(32)	-	-	-	117.85812 / 117.88920	121.06720 / 120.93603
C(34)-C(38)-C(39)	-	-	-	120.95201 / 120.89916	119.45826 / 119.52603
C(39)-C(38)-C(32)	-	-	-	121.18188 / 121.20378	-
C(38)-C(39)-H(41)	-	-	-	111.43306 / 111.19182	-
H(40)-C(39)-C(38)	-	-	-	111.41971 / 111.22471	-
C(38)-C(32)-C(30)	-	-	-	121.09653 / 121.06302	119.04081 / 119.16149
C(38)-C(32)-H(36)	-	-	-	119.49359 / 119.68378	120.15811 / 120.17011
H(41)-C(39)-H(42)	-	-	-	107.30979 / 107.68553	-
H(42)-C(39)-H(40)	-	-	-	107.46650 / 107.75764	-
H(36)-C(32)-C(30)	-	-	-	119.40941 / 119.25285	120.80098 / 120.66833
Cl(39)-C(38)-C(32)	-	-	-	-	119.47434 / 119.53777

Table 2 – The calculated bond lengths (Å) of all molecules as DFT (B3LYP) and HF (B3LYP) methods on the basis set of 6-311G (d,p).

Bond Lengths (Å)	Molecule 1	Molecule 2	Molecule 3	Molecule 4	Molecule 5
	DFT / HF				
N(1)-H(7)	1.00581 / 0.99044	1.00576 / 0.99039	1.00586 / 0.99046	1.00582 / 0.99043	1.00597 / 0.99058
N(1)-N(3)	1.38360 / 1.37314	1.38340 / 1.37294	1.38302 / 1.37226	1.38325 / 1.37249	1.38247 / 1.37175
N(3)=C(25)	1.29459 / 1.26497	1.29446 / 1.26525	1.29349 / 1.26403	1.29345 / 1.26412	1.29343 / 1.26394
C(25)-C(26)	1.48540 / 1.48752	1.49287 / 1.49410	1.49834 / 1.49862	1.49850 / 1.49882	1.49847 / 1.49859
C(26)-H(28)	1.08908 / 1.08062	1.09593 / 1.08637	1.09509 / 1.08515	1.09504 / 1.08521	1.09479 / 1.08496
C(26)-H(27)	1.09304 / 1.08408	-	1.09558 / 1.08536	1.09587 / 1.08553	1.09561 / 1.08524
C(26)-C(27)	-	1.52977 / 1.52560	-	-	-
C(27)-H(30)	-	1.09173 / 1.08450	-	-	-
C(27)-H(31)	-	1.09124 / 1.08352	-	-	-
C(27)-H(32)	-	1.09124 / 1.08342	-	-	-
C(26)-H(29)	1.09315 / 1.08425	1.09594 / 1.08623	-	-	-
C(25)-N(4)	1.39016 / 1.38192	1.39131 / 1.38321	1.39185 / 1.38423	1.39219 / 1.38452	1.39088 / 1.38324
N(4)-C(2)	1.41673 / 1.38767	1.41643 / 1.38722	1.41641 / 1.38716	1.41647 / 1.38702	1.41728 / 1.38768
C(2)=O(5)	1.21146 / 1.19112	1.21156 / 1.19129	1.21164 / 1.19130	1.21179 / 1.19145	1.21112 / 1.19076
C(2)-N(1)	1.36895 / 1.34799	1.36904 / 1.34665	1.36885 / 1.34656	1.36869 / 1.34641	1.36927 / 1.34709
N(4)-N(6)	1.37300 / 1.36147	1.37277 / 1.36144	1.37316 / 1.36172	1.37305 / 1.36168	1.37354 / 1.36196
N(6)-H(8)	1.01460 / 0.99815	1.01446 / 0.99810	1.01469 / 0.99823	1.01460 / 0.99821	1.01478 / 0.99835
N(6)-C(9)	1.40482 / 1.39490	1.40384 / 1.39432	1.40516 / 1.39519	1.40460 / 1.39488	1.40635 / 1.39633
C(9)=O(10)	1.20647 / 1.18229	1.20675 / 1.18245	1.20642 / 1.18222	1.20656 / 1.18231	1.20608 / 1.18186
C(9)-C(11)	1.52568 / 1.51818	1.52565 / 1.51823	1.52566 / 1.51820	1.52568 / 1.51822	1.52546 / 1.51810
C(11)-H(24)	1.08979 / 1.08622	1.08962 / 1.08622	1.08985 / 1.08612	1.08983 / 1.08612	1.08989 / 1.08611
C(11)-H(23)	1.09538 / 1.08341	1.09536 / 1.08337	1.09537 / 1.08346	1.09532 / 1.08343	1.09537 / 1.08356
C(11)-C(12)	1.51419 / 1.51016	1.51420 / 1.51016	1.51440 / 1.51012	1.51430 / 1.51011	1.51434 / 1.51014
C(12)-C(15)	1.39873 / 1.38916	1.39860 / 1.38916	1.39876 / 1.38902	1.39876 / 1.38905	1.39870 / 1.38896
C(15)-H(20)	1.08505 / 1.07538	1.08503 / 1.07537	1.08508 / 1.07542	1.08509 / 1.07542	1.08509 / 1.07544
C(15)=C(13)	1.39226 / 1.38193	1.39237 / 1.38195	1.39226 / 1.38204	1.39221 / 1.38204	1.39218 / 1.38207
C(13)-H(21)	1.08435 / 1.07542	1.08435 / 1.07542	1.08436 / 1.07541	1.08436 / 1.07542	1.08432 / 1.07539

Table continuation

Bond Lengths (Å ⁰)	Molecule 1	Molecule 2	Molecule 3	Molecule 4	Molecule 5
	DFT / HF				
C(13)-C(14)	1.39374 / 1.38637	1.39368 / 1.38636	1.39381 / 1.38627	1.39386 / 1.38627	1.39386 / 1.38623
C(14)-H(22)	1.08429 / 1.07538	1.08430 / 1.07539	1.08428 / 1.07538	1.08429 / 1.07538	1.08426 / 1.07535
C(14)=C(16)	1.39252 / 1.38211	1.39267 / 1.38213	1.39250 / 1.38222	1.39247 / 1.38221	1.39245 / 1.38225
C(16)-H(19)	1.08435 / 1.07552	1.08436 / 1.07553	1.08435 / 1.07552	1.08436 / 1.07552	1.08433 / 1.07549
C(16)-C(17)	1.39311 / 1.38634	1.39293 / 1.38633	1.39309 / 1.38622	1.39312 / 1.38624	1.39313 / 1.38617
C(17)-H(18)	1.08479 / 1.07668	1.08472 / 1.07668	-	1.08481 / 1.07670	1.08482 / 1.07673
C(17)=C(12)	1.39569 / 1.38578	1.39578 / 1.38581	-	1.39564 / 1.38585	1.39559 / 1.38584
C(26)-C(29)	-	-	1.51333 / 1.51237	1.51274 / 1.51178	1.51261 / 1.51185
C(29)-C(31)	-	-	1.39664 / 1.38704	1.39629 / 1.38686	1.39607 / 1.38635
C(31)-H(35)	-	-	1.08514 / 1.07633	1.08526 / 1.07656	1.08464 / 1.07579
C(31)-C(34)	-	-	1.39216 / 1.38398	1.39059 / 1.38231	1.39137 / 1.38305
C(34)-H(38)	-	-	1.08417 / 1.07537	-	-
C(34)-C(36)	-	-	1.39321 / 1.38434	-	-
C(36)-H(39)	-	-	1.08407 / 1.07527	-	-
C(36)-C(32)	-	-	1.39283 / 1.38417	-	-
C(32)-C(37)	-	-	1.08419 / 1.07536	-	-
C(32)-C(30)	-	-	1.39263 / 1.38418	1.39216 / 1.38447	1.39173 / 1.38334
C(30)-H(33)	-	-	1.08522 / 1.07626	1.08537 / 1.07648	1.08475 / 1.07574
C(30)-C(29)	-	-	1.39627 / 1.38687	1.39489 / 1.38482	1.39587 / 1.38612
C(32)-H(36)	-	-	-	1.08528 / 1.07624	1.08223 / 1.07324
C(32)-C(38)	-	-	-	1.39719 / 1.38735	1.38995 / 1.38028
C(38)-C(39)	-	-	-	1.50963 / 1.51034	-
C(39)-H(40)	-	-	-	1.09212 / 1.08418	-
C(39)-H(41)	-	-	-	1.09278 / 1.08473	-
C(39)-H(42)	-	-	-	1.09548 / 1.08702	-
C(38)-C(34)	-	-	-	1.39884 / 1.38946	1.39027 / 1.38054
C(34)-H(37)	-	-	-	1.08542 / 1.07644	1.08222 / 1.07324
C(38)-Cl(39)	-	-	-		1.75963 / 1.74441

Quantifying the distribution of electronic charge among the atoms in a molecule is the Mulliken atomic charge, which is a notion from quantum chemistry. This technique uses a quantum mechanical computation to take into account the overlap of atomic orbitals and their contributions to molecular orbitals in order to estimate the charge distribution on individual atoms within a molecule. The estimation of charge distributions inside molecules and comprehension of their chemical activity have traditionally been accomplished using mulliken atomic charges. Mulliken atomic charge values of the studied molecules in this article are given in Table 3. When the Mulliken atomic charge

values given in Table 3 were examined, it was determined that the highest value was calculated as 0.6880 in the C2 atom of the 2nd molecule according to the HF model, and the lowest value was calculated as -0.5025 in the O2 atom of the 4th molecule according to the HF model.

In quantum chemistry, the words HOMO and LUMO are used to characterize particular energy levels inside the electronic structure of molecules. They are essential for comprehending the electrical, bonding, and reactivity characteristics of molecules. The HOMO (Highest Occupied Molecular Orbital) is the highest energy molecular orbital that contains electrons.

Table 3 – Mulliken atomic charge values of the studied molecules according to DFT (B3LYP) and HF (B3LYP) methods on the basis set of 6-311G (d,p).

Molecule														
1			2			3			4			5		
Atom	DFT	HF	Atom	DFT	HF	Atom	DFT	HF	Atom	DFT	HF	Atom	DFT	HF
N1	-0.3023	-0.3683	N1	-0.3017	-0.3699	N1	-0.3026	-0.3695	N1	-0.3025	-0.3695	N1	-0.3022	-0.3694
C2	0.4984	0.6875	C2	0.4983	0.6880	C2	0.4990	0.6870	C2	0.4989	0.6868	C2	0.4999	0.6877
N3	-0.2158	-0.2762	N3	-0.2255	-0.2835	N3	-0.2046	-0.2597	N3	-0.2049	-0.2601	N3	-0.2052	-0.2599
N4	-0.3813	-0.4743	N4	-0.3909	-0.4859	N4	-0.3907	-0.4850	N4	-0.3906	-0.4850	N4	-0.3909	-0.4853
O5	-0.3674	-0.5011	O5	-0.3679	-0.2018	O5	-0.3682	-0.5018	O5	-0.3688	-0.5025	O5	-0.3658	-0.4993
N6	-0.2699	-0.3299	N6	-0.2689	-0.3286	N6	-0.2681	-0.3294	N6	-0.2682	-0.3291	N6	-0.2699	-0.3307
H7	0.2546	0.2639	H7	0.2541	0.2634	H7	0.2550	0.2645	H7	0.2545	0.2640	H7	0.2564	0.2659
H8	0.2478	0.2572	H8	0.2476	0.2568	H8	0.2475	0.2570	H8	0.2474	0.2568	H8	0.2481	0.2576
C9	0.3869	0.5478	C9	0.3885	0.5480	C9	0.3867	0.5477	C9	0.3867	0.5478	C9	0.3862	0.5472
O10	-0.3223	-0.4268	O10	-0.3236	-0.4276	O10	-0.3220	-0.4263	O10	-0.3226	-0.4269	O10	-0.3201	-0.4243
C11	-0.2739	-0.2544	C11	-0.2749	-0.2548	C11	-0.2747	-0.2547	C11	-0.2739	-0.2546	C11	-0.2738	-0.2546
C12	-0.0931	-0.0648	C12	-0.0937	-0.0651	C12	-0.0934	-0.0642	C12	-0.0938	-0.0643	C12	-0.0933	-0.0638
C13	-0.0994	-0.0806	C13	-0.0992	-0.0807	C13	-0.0995	-0.0803	C13	-0.0998	-0.0804	C13	-0.0995	-0.0800
C14	-0.0851	-0.1035	C14	-0.0854	-0.1036	C14	-0.0851	-0.1035	C14	-0.0851	-0.1036	C14	-0.0847	-0.1031
C15	-0.0486	-0.0692	C15	-0.0482	-0.0692	C15	-0.0484	-0.0701	C15	-0.0487	-0.0700	C15	-0.0492	-0.0705
C16	-0.0941	-0.0776	C16	-0.0941	-0.0777	C16	-0.0939	-0.0776	C16	-0.0939	-0.0776	C16	-0.0933	-0.0773
C17	-0.0555	-0.0909	C17	-0.0542	-0.0909	C17	-0.0558	-0.0906	C17	-0.0561	-0.0906	C17	-0.0564	-0.0905
H18	0.0799	0.0808	H18	0.0800	0.0809	H18	0.0800	0.0803	H18	0.0799	0.0805	H18	0.0801	0.0794
H19	0.0921	0.0966	H19	0.0921	0.0964	H19	0.0921	0.0967	H19	0.0919	0.0966	H19	0.0927	0.0972
H20	0.1155	0.0943	H20	0.1142	0.0943	H20	0.1162	0.0943	H20	0.1169	0.0943	H20	0.1169	0.0946
H21	0.1155	0.0999	H21	0.0936	0.0999	H21	0.0938	0.1000	H21	0.0937	0.0999	H21	0.0944	0.1006
H22	0.0926	0.0979	H22	0.0936	0.0977	H22	0.0926	0.0979	H22	0.0924	0.0978	H22	0.0932	0.0986
H23	0.1479	0.1333	H23	0.1333	0.1335	H23	0.1475	0.1321	H23	0.1472	0.1324	H23	0.1473	0.1309
H24	0.1435	0.1737	H24	0.1483	0.1736	H24	0.1433	0.1739	H24	0.1435	0.1738	H24	0.1431	0.1743
C25	0.3002	0.3919	C25	0.3566	0.4637	C25	0.3656	0.4743	C25	0.3656	0.4748	C25	0.3655	0.4742
C26	-0.2515	-0.1837	C26	-0.2156	-0.1929	C26	-0.1944	-0.1448	C26	-0.1949	-0.1475	C26	-0.1916	-0.1421

Table continuation

Molecule														
1			2			3			4			5		
Atom	DFT	HF	Atom	DFT	HF	Atom	DFT	HF	Atom	DFT	HF	Atom	DFT	HF
H27	0.1318	0.1228	C27	-0.2863	-0.2215	H27	0.1458	0.1399	H27	0.1453	0.1393	H27	0.1479	0.1424
H28	0.1318	0.1354	H28	0.1346	0.1204	H28	0.1418	0.1423	H28	0.1405	0.1412	H28	0.1438	0.1446
H29	0.1334	0.1183	H29	0.1324	0.1241	C29	-0.0936	-0.0913	C29	-0.0882	-0.1017	C29	-0.0936	-0.1003
			H30	0.1120	0.0980	C30	-0.0528	-0.0781	C30	-0.0549	-0.0581	C30	-0.0510	-0.0629
			H31	0.1213	0.1067	C31	-0.0479	-0.0776	C31	-0.0468	-0.0565	C31	-0.0449	-0.0617
			H32	0.1214	0.1081	C32	-0.0907	-0.0771	C32	-0.0706	-0.0833	C32	0.0259	0.0275
						H33	0.0839	0.0863	H33	0.0813	0.0843	H33	0.0925	0.0954
						C34	-0.0909	-0.0776	C34	-0.0743	-0.0879	C34	0.0254	0.0268
						H35	0.0836	0.0848	H35	0.0809	0.0829	H35	0.0921	0.0954
						C36	-0.0872	-0.1026	H36	0.0852	0.0889	H36	0.1203	0.1274
						H37	0.0964	0.1009	H37	0.0855	0.0889	H37	0.1204	0.1273
						H38	0.0966	0.1008	C38	-0.0967	-0.1208	C38	-0.2369	-0.2186
						H39	0.0970	0.1008	H40	0.1109	0.0972	CI39	-0.0691	-0.0994
									H41	0.1158	0.1078			
									H42	0.1289	0.1152			

In other words, it's the orbital where the last electron is placed when building up the electron configuration of a molecule. The HOMO is important because it determines how a molecule can interact with other molecules or undergo chemical reactions. Electrons in the HOMO are more readily available for participating in chemical reactions, such as bond formation or electron transfer.

The LUMO (Lowest Unoccupied Molecular Orbital) is the lowest energy molecular orbital that is devoid of electrons. It stands for the level of energy that is available after the HOMO. Because it shows the energy needed to remove an electron from a molecule or the energy obtained when an electron is supplied to the molecule, the LUMO is important. It is more likely for molecules with accessible,

low-energy LUMOs to take electrons or engage in electron transfer reactions. When the HOMO and LUMO values given in Figure 2-6 were examined, it was determined that the highest HOMO value was calculated as $E_{HOMO} = 0.12572$ in the 1st molecule according to the HF method, and the lowest value was calculated as $E_{HOMO} = -0.33409$ in the 5th molecule according to the HF method. In LUMO values, it was determined that the highest value was calculated as $E_{LUMO} = 0.11845$ in the 4th molecule according to the HF method, and the lowest value was calculated as $E_{LUMO} = -0.33166$ in the 1st molecule according to the HF method. The HOMO-LUMO gap, or the energy difference between the HOMO and LUMO, is crucial in determining a molecule's optical and electrical properties.

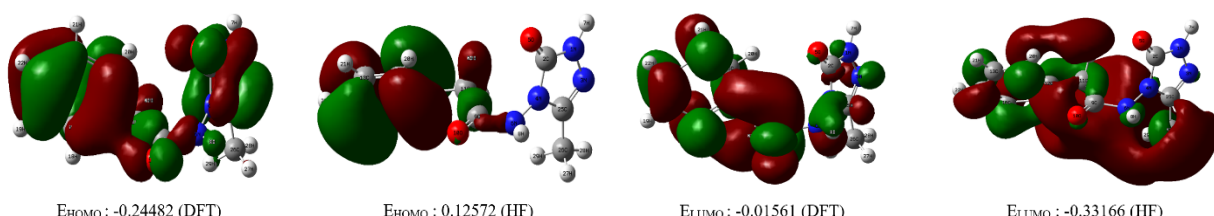


Figure 2 – The calculated HOMO-LUMO energies of molecule 1 according to DFT/B3LYP/6-311G (d,p) and HF/6-311G (d,p) levels

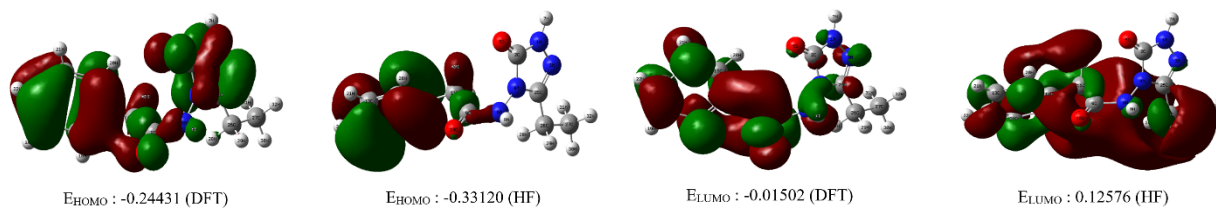


Figure 3 – The calculated HOMO-LUMO energies of molecule 2 according to FT/B3LYP/6-311G (d,p) and HF/6-311G (d,p) levels

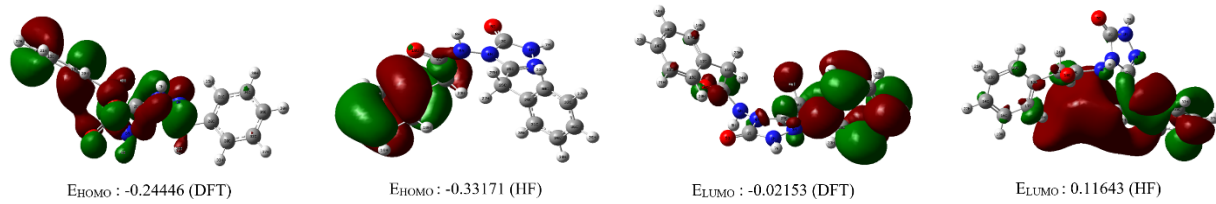


Figure 4 – The calculated HOMO-LUMO energies of molecule 3 according to DFT/B3LYP/6-311G (d,p) and HF/6-311G (d,p) levels

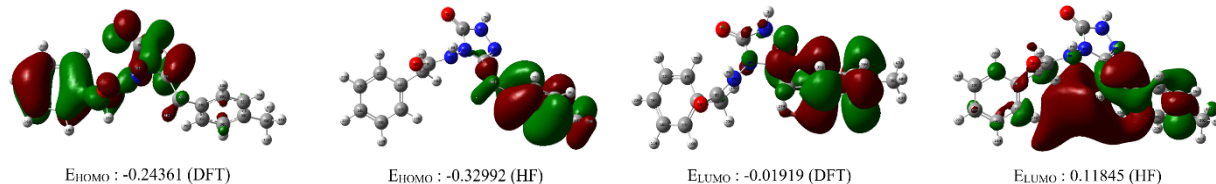


Figure 5 – The calculated HOMO-LUMO energies of molecule 4 according to DFT/B3LYP/6-311G (d,p) and HF/6-311G (d,p) levels

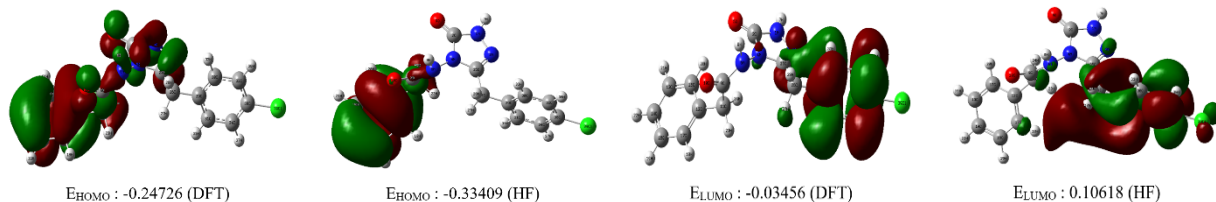


Figure 6 – The calculated HOMO-LUMO energies of molecule 5 according to DFT/B3LYP/6-311G (d,p) and HF/6-311G (d,p) levels

Chemistry uses the phrases “dipole moment” and “total energy” to define crucial aspects of molecules, notably in relation to molecular structure, polarity, and stability. Due to variations in atom electronegativity, a dipole moment is a measurement of the separation of positive and negative charges within a molecule. In other words, it measures the level of polarity or charge imbalance within a molecule. An electron dipole molecule has a positive

end (where there are fewer electrons) and a negative end (where there are more electrons). It is possible to visualize the dipole moment as a vector quantity with magnitude and direction. The highest dipole moment was calculated as $\mu_{\text{Total}} = 4.6286$ debye in the 4th molecule according to the HF technique, and the lowest dipole moment was calculated as $\mu_{\text{Total}} = 1.9017$ debye in the 5th molecule according to the HF method, according to the data presented in Table 4.

Table 4 – Dipole moment (debye) and total energy (a.u.) values

Molecule	Property		DFT	HF
1	Dipole Moment	μ_x	2.9971	-1.8265
		μ_y	-0.7008	3.2453
		μ_z	-2.1778	-1.0955
		μ_{Total}	3.7705	3.8818
	Total Energy		-796.04737247	-791.24048825
2	Dipole Moment	μ_x	3.3650	-2.3642
		μ_y	-0.7446	3.1523
		μ_z	-1.9495	-1.1001
		μ_{Total}	3.9596	4.0911
	Total Energy		-835.37126756	-830.28438620
3	Dipole Moment	μ_x	3.7860	3.5073
		μ_y	-0.7885	-2.1527
		μ_z	-1.2606	-0.8062
		μ_{Total}	4.0675	4.1935
	Total Energy		-1027.14715452	-1020.82813853
4	Dipole Moment	μ_x	4.2768	4.0775
		μ_y	-0.8039	-2.0416
		μ_z	-1.2495	-0.7937
		μ_{Total}	4.5275	4.6286
	Total Energy		-1066.47482216	-1059.87421405
5	Dipole Moment	μ_x	1.7914	1.5602
		μ_y	-0.5104	-1.0774
		μ_z	-0.4160	-0.1468
		μ_{Total}	1.9086	1.9017
	Total Energy		-1486.76855799	-1479.74965931

The sum of all the energy contributions made by a molecule's different parts, such as the electronic energy (energy of electrons), nuclear repulsion energy (caused by the positive charges of the atomic nuclei repelling one another), and other potential and kinetic energy terms, makes up the total energy of the molecule. A crucial characteristic that governs a molecule's stability and behavior is its total energy. The total energy of a molecule can be determined in quantum mechanics using techniques like the Hartree-Fock theory, density functional theory (DFT), or more sophisticated ab initio techniques. The stability of various molecular conformations, the

strength of chemical bonds, and the energy changes brought on by chemical reactions are all factors that can be understood by energy calculations. When the total energy values are examined in the same Table 4, it appears to be calculated the highest total energy is -791.24048825 a.u. in the 1st molecule according to the HF method and, the lowest total energy is -1486.76855799 a.u. in the 5th molecule according to the DFT method. All dipole moment and total energy values for studied compounds according to DFT/B3LYP/6-311G (d,p) and HF/6-311G (d,p) levels were given in Table 4. The graphical submission of these values is given on Figures 7-8.

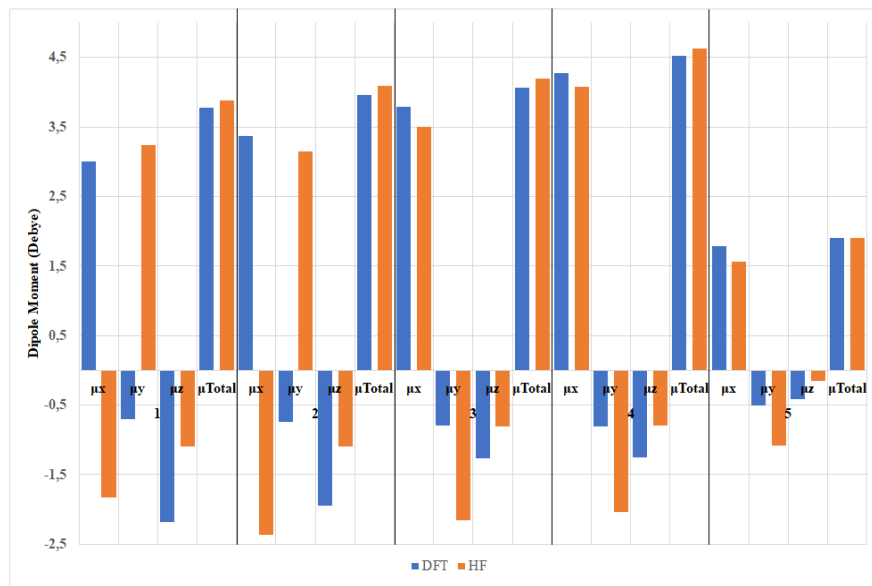


Figure 7 – Graphical submission of dipole moment values of studied molecules

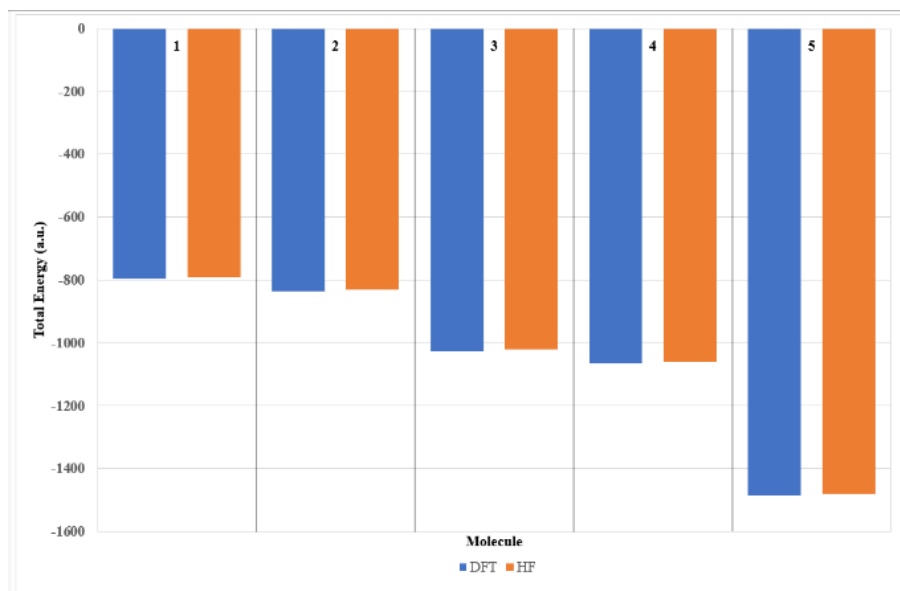


Figure 8 – Graphical submission of total energy values of studied molecules

IR spectrum analysis is the process of studying and analyzing the interaction between matter and infrared light using infrared (IR) spectroscopy. In order to recognize and describe the functional groups, chemical bonds, and molecular structures contained in a sample, IR spectroscopy is a technique that is frequently employed in chemistry, physics, and numerous other scientific disciplines. Longer wavelengths than visible light allow infrared light to interact with molecules' vibrational states. Every molecule contains unique

vibrational frequencies, such as ν : stretching vibration, δ : bending vibration, γ : out-of plane bending vibration, τ : torsion vibration, connected to the motion of its atoms. It has been determined that the spectra obtained from these values and given in Figure 5-14 are compatible with each other with "vibration types and IR frequencies (cm^{-1})" values of molecules calculated according to DFT and HF methods and given in Table 5-9. The IR spectrum obtained from these values is also given on Figures 9-18.

Table 5 – Vibration types and IR frequencies (cm^{-1}) of molecule 1

Seq.	Vibration Types	DFT	HF
1	τ CCCC(46), τ CNNN(21), τ NCCC(12)	30	16
2	τ CCCC(33), τ CNNC(31)	34	32
3	τ NNCC(31), τ CCCC(15), τ NNC(13), τ NCCC(12)	42	54
4	τ NNCC(15), τ CNNC(30), δ NNC(10)	61	74
5	τ NCNN(62)	75	85
6	τ NNCC(12), γ CCCC(16), γ CNNC(19), δ CCC(19)	102	105
7	γ CCCC(12), γ CNNC(10), τ NNCC(12), τ HCCN(11)	133	140
8	τ HCCN(17), τ NCCC(23)	148	165
9	δ NCC(11), δ CCC(10), δ NNC(12)	243	249
10	δ NCC(15), δ CCC(23), τ CCCC(17)	249	274
11	δ CCN(45)	267	288
12	γ CCCC(19), γ CNNC(17), τ NNCN(14)	307	325
13	δ CNN(30)	312	354
14	δ OCN(14)	321	362
15	δ CCC(20), δ CCC(31)	343	452
16	τ HCCC(12), τ CCCC(42)	417	480
17	δ OCN(11), ν NC(12), ν NN(12)	441	492
18	δ OCN(10), τ HNNC(28)	467	503
19	τ HNNC(40)	471	537
20	τ CCCC(18)	496	579
21	γ ONNC(11), γ OCNC(15), τ HNNC(14)	534	643
22	τ HNNC(13), δ OCN(12), δ CCC(19)	583	667
23	δ CNN(18), δ CCN(12), δ OCN(14)	596	679
24	δ CCC(49)	637	707
25	ν CC(13), ν NN(12), δ CNN(11), δ OCN(11)	645	715
26	τ NNCN(42)	665	745
27	γ ONNC(13), γ OCNC(10), τ CCCC(12)	700	771
28	τ HCCC(10), τ CCCC(11), τ HCCC(28)	717	815
29	τ HCCC(46), ν CC(12)	750	868
30	γ ONNC(41), γ OCNC(39)	758	870
31	δ CNN(20), δ NNC(22)	804	893
32	ν CC(14)	830	921
33	τ HCCC(59)	860	946
34	δ NCN(11), ν NC(16)	900	993
35	τ HCCC(14), τ HCCN(10), τ HCCC(26), τ HCCN(10)	935	1021
36	τ HCCN(12), τ HCCC(16)	950	1046
37	τ HCCC(22), τ CCCC(18), τ HCCC(10)	983	1085
38	δ NNC(23), τ HCCN(16)	993	1087
39	τ HCCC(12), τ CCCC(18), τ HCCC(53)	1005	1095
40	δ CCC(56), ν CC(33)	1019	1115
41	δ HCC(18), δ CCC(10), ν CC(23)	1054	1121
42	δ CNN(10), ν NC(13), ν NN(35)	1057	1163

Table continuation

Seq.	Vibration Types	DFT	HF
42	τ HCCN(16), τ HCCN(25), δ HCH(10)	1067	1169
43	ν NN(27)	1100	1171
44	δ HCC(14), ν CC(25), ν CC(17), δ HCC(11)	1106	1191
45	δ HCC(33)	1174	1199
46	ν CC(12), δ HCC(65)	1183	1215
47	δ HCC(36), δ HCC(13), ν CC(10)	1209	1250
48	ν CC(13)	1218	1290
49	δ OCN(14), ν NC(18)	1233	1294
50	ν NN(17)	1238	1308
51	δ HCC(20), ν CC(13), ν NC(10)	1250	1334
52	δ NCN(19)	1328	1358
53	δ HCC(10), ν CC(27), ν CC(11), ν CC(16)	1339	1371
54	τ HCCN(25)	1359	1460
55	δ HCC(51), δ HCC(25)	1368	1471
56	δ HCH(11), δ HNN(65)	1397	1519
57	ν NN(12), δ HCH(51)	1422	1538
58	ν NC(19), ν NN(19), δ HNC(13)	1450	1559
59	δ HCH(29), δ HNC(42)	1467	1590
60	δ HNC(14), δ HCH(35)	1474	1591
61	τ HCCN(13), δ HCH(45)	1476	1593
62	δ HCC(21), ν CC(12)	1488	1604
63	δ HCH(29)	1491	1629
64	δ HCC(31), δ HCC(18), δ CCC(10)	1532	1639
65	δ CCC(12), ν CC(40)	1630	1656
66	δ HCC(12), ν CC(20)	1649	1772
67	ν NC(67)	1656	1798
68	ν OC(59)	1805	1873
69	ν NC(10), ν OC(54)	1834	1982
70	ν CH(14), ν CH(41)	3042	2001
71	ν CH(52), ν CH(25)	3043	3191
72	ν CH(49), ν CH(13)	3094	3198
73	ν CH(39)	3112	3244
74	ν CH(36)	3144	3250
75	ν CH(93)	3158	3293
76	ν CH(63), ν CH(27)	3164	3310
77	ν CH(44), ν CH(39)	3172	3320
78	ν CH(52), ν CH(22)	3180	3331
79	ν CH(85)	3189	3341
80	ν NH(50)	3538	3351
81	ν NH(50)	3682	3800

Note: ν : stretching vibration, δ : bending vibration, γ : out-of plane bending vibration, τ : torsion vibration

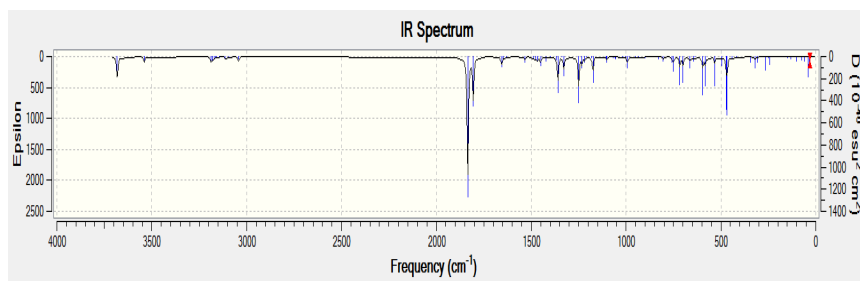


Figure 9 – Theoretical IR spectrums according to DFT/B3LYP/6-311G (d,p) level for molecule 1

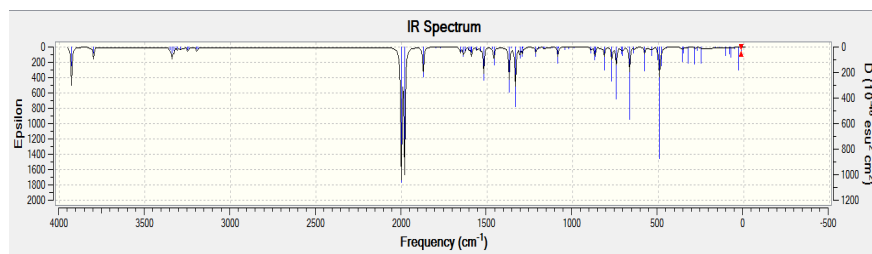


Figure 10 – Theoretical IR spectrums according to HF/B3LYP/6-311G (d,p) level for molecule 1.

Table 6 – Vibration types and IR frequencies (cm^{-1}) of molecule 2

Seq.	Vibration Types	DFT	HF
1	τ CCCC(70)	16	16
2	τ CCCC(18), τ CNNC(21), τ NCCC(29)	27	27
3	τ CNNC(55), τ CCCN(13)	32	48
4	τ NCNN(12), τ CNNC(15), τ CCCN(32), τ NNCC(38)	57	66
5	τ NCNN(54)	80	76
6	δ CCC(17), γ CCCC(14), γ CNNC(21), τ NNCC(12)	101	79
7	τ CNNC(13), τ NCCN(17), τ NNCN(11), γ CCCC(16), γ CNNC(12)	131	105
8	δ CCN(52), δ CCC(25)	176	134
9	τ HCCC(9)	214	192
10	δ CCC(11), τ CCCC(20)	248	232
11	τ CNNC(15), δ NCC(24), δ CCC(12)	255	257
12	δ CNN(17), δ CCC(12)	302	275
13	τ NNCN(13), γ CCCC(11)	310	325
14	δ CCC(19), δ CCC(11), δ OCN(10)	338	334
15	δ NCC(11), δ CCC(14), δ CCC(10), δ OCN(11)	345	358
16	τ CCCC(42), τ HCCC(13)	415	375
17	δ OCN(11), τ HNNC(27), δ OCN(14), ν NN(10)	467	452
18	τ NNCN(10), τ HNNC(42)	470	483
19	τ CCCC(17)	496	492
20	γ ONNC(14), γ OCNC(10), τ HNNC(16)	533	536
21	δ CCC(22), τ HNNC(10), τ HNCC(15)	582	578
22	δ CCC(24), δ CCC(49)	637	653
23	τ NNCN(42), τ CCCN(11)	657	679

Table continuation

Seq.	Vibration Types	DFT	HF
24	δ CCN(15), δ CCC(16), ν CC(10)	672	708
25	γ ONNC(10), γ OCNC(13)	698	718
26	τ CCCC(11;36), τ HCCC(29), τ HCCC(10)	716	741
27	ν CC(13), τ HCCC(45)	750	771
28	γ ONNC(40), γ OCNC(40)	757	815
29	δ CNN(11;31), δ NNC(13)	797	859
30	τ HCCN(17;16), τ HCCN(16;15;14)	803	863
31	ν CC(16;11)	832	876
32	τ HCCC(16)	855	896
33	τ HCCC(50), τ HCCC(22)	858	921
34	δ NCN(12), γ NC(16)	904	946
35	τ HCCC(28), τ HCCC(15)	935	996
36	τ HCCC(14), τ HCCC(10;11), δ NNC(19), ν CC(49)	949	1021
37	τ CCCC(18), τ HCCC(10;23), τ HCCC(23), τ HCCC(17)	981	1041
38	τ CCCC(17), τ HCCC(53), τ HCCC(12)	1004	1047
39	δ CCC(57), ν CC(33)	1019	1085
40	δ NNC(20), δ CCC(13)	1039	1095
41	δ CCC(10), δ HCC(13), ν CC(13;24)	1053	1115
42	ν NN(42), ν CC(17)	1073	1121
42	δ HCC(28), ν CC(25), ν CC(16)	1106	1135
43	τ HCCC(14), ν NN(18), ν CC(15), δ HCH(10)	1111	1169
44	τ HCCN(18), τ HCCC(21), δ HCH(12)	1115	1175
45	δ HCC(18;17)	1174	1199
46	δ HCC(15;12), δ HCC(44), ν CC(13)	1183	1211
47	δ HCC(40), δ HCC(15)	1208	1218
48	ν CC(35)	1219	1290
49	ν NC(19;20), ν NN(10), δ OCN(14)	1231	1294
50	ν NC(10), ν CC(12), δ HCC(10;14)	1251	1309
51	δ HCC(28;24)	1288	1335
52	δ CNN(11), δ NCN(13)	1292	1358
53	ν CC(11;27), ν CC(16)	1339	1368
54	τ HCCN(19;30)	1357	1395
55	δ HCC(15;16), δ HCC(24)	1367	1416
56	τ HCCN(28), δ HNC(17), ν NN(10)	1378	1471
57	δ HNC(55), ν NN(11)	1403	1513
58	δ HCH(95)	1422	1521
59	ν NC(18), ν NN(20), δ HNC(19)	1454	1545
60	δ HNC(33), δ HCH(39)	1470	1556
61	δ HCH(44;16), δ HNC(20)	1476	1591
62	δ HCH(31;24)	1480	1597
63	ν CC(13), δ HCC(41)	1488	1604
64	τ HCCC(12;11), δ HCH(75)	1496	1611
65	τ HCCC(10), δ HCH(63)	1509	1617

Table continuation

Seq.	Vibration Types	DFT	HF
66	δ CCC(10), δ HCC(38), δ HCC(18)	1532	1630
67	δ CCC(12), v CC(39;11), δ HCC(11)	1629	1638
68	v NC(48)	1648	1656
69	v CC(12;14), v NC(20)	1649	1772
70	v OC(27)	1804	1798
71	v OC(59)	1805	1865
72	v OC(21;53)	1834	1981
73	v CH(51;49)	3025	2000
74	v CH(38;15;40)	3043	3181
75	v CH(44;52)	3046	3186
76	v CH(96)	3048	3198
77	v CH(11;39)	3114	3210
78	v CH(45;50)	3115	3244
79	v CH(51;46)	3119	3249
80	v CH(11;39)	3144	3260
81	v CH(93)	3158	3310
82	v CH(63), v CH(28)	3164	3320
83	v CH(43;18), v CH(38)	3172	3331
84	v CH(52;15), v CH(22)	3179	3341
85	v CH(85)	3189	3351
86	v NH(50)	3540	3800
87	v NH(50)	3681	3929

Note: v: stretching vibration, δ : bending vibration, y: out-of plane bending vibration, τ : torsion vibration

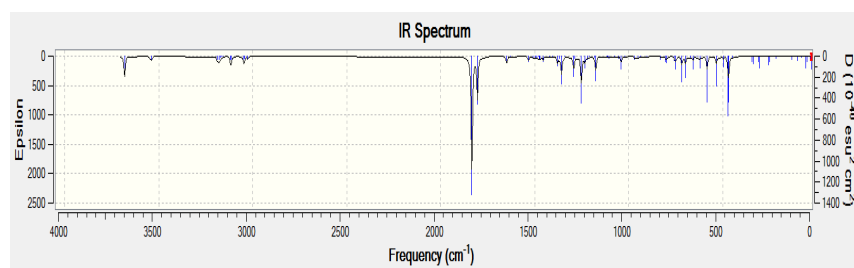


Figure 11 – Theoretical IR spectrums according to DFT/B3LYP/6-311G (d,p) level for molecule 2

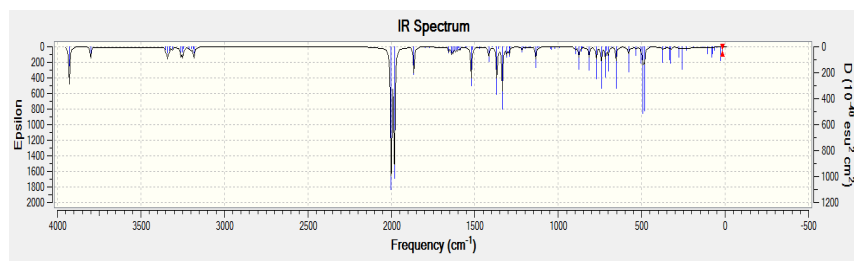


Figure 12 – Theoretical IR spectrums according to HF/B3LYP/6-311G (d,p) level for molecule 2

Table 7 – Vibration types and IR frequencies (cm^{-1}) of molecule 3

Seq.	Vibration Types	DFT	HF
1	τ CNNC(41), τ NCCN(38)	13	13
2	τ CNNC(15), τ CCCN(61)	23	23
3	τ CCCN(13), τ CCCC(59)	29	29
4	τ CCCC(84)	32	37
5	τ CCNN(33)	39	44
6	τ CNNC(45)	43	59
7	γ CCCC(29), δ CCC(19)	71	75
8	τ NNCC(64)	78	84
9	τ CCNN(15), τ CCCC(14;10), δ CCC(16;13)	101	112
10	γ NCNC(18), τ NNCC(43;12)	128	139
11	δ NCC(40)	185	196
12	τ CCCC(17;13), ν CC(12)	235	249
13	τ CCCC(34;13), δ CCC(12)	248	256
14	δ CCN(29), δ CCC(17)	251	287
15	γ NCNC(10), τ NNCC(21), τ CNNC(15;22)	294	305
16	δ NNC(25), δ OCN(15)	324	326
17	δ CCC(28)	333	339
18	δ CCC(51)	341	367
19	τ CCCC(77)	414	421
20	τ CCCC(48;15)	415	423
21	ν NC(11), ν NN(14)	428	446
22	τ HNNC(27), δ OCN(10)	466	486
23	γ NCNC(10), τ HNNC(46)	471	490
24	γ CCCC(18), τ CCCC(21)	484	496
25	τ CCCC(20;13)	497	521
26	γ ONNC(12;16), τ HNNC(14)	535	542
27	δ OCN(18), δ CCC(27)	566	573
28	τ HNNC(16;10), δ CCC(20)	586	605
29	δ NNC(12), δ OCN(19), δ CCC(17)	632	642
30	δ CCC(48;15)	636	648
31	δ CCC(53;23), δ CCC(15;11)	637	657
32	γ NCNC(39), τ HNNC(10)	660	669
33	τ CCCC(12)	698	708
34	τ CCCC(29)	704	716
35	τ CCCC(10), τ HCCC(17), τ HCCC(52)	715	734
36	τ CCCC(21;12), τ HCCC(10), τ HCCC(29)	717	745
37	τ CCCC(12), τ HCCC(43)	750	763
38	γ ONNC(40;41)	758	776
39	τ CCCC(11), τ HCCC(13), δ CNN(16)	780	798
40	δ NNC(12), δ CNN(10)	805	824
41	ν CC(26)	830	442
42	τ HCCC(26)	835	849

Table continuation

Seq.	Vibration Types	DFT	HF
42	v CC(18)	843	857
43	τ HCCC(54)	853	861
44	τ HCCC(16)	855	865
45	τ HCCC(22), τ HCCC(50)	859	879
46	v NC(14), δ OCN(10)	906	925
47	τ HCCN(10;11), δ HCC(13)	930	938
48	τ HCCN(15), τ HCCC(18), τ HCCC(17)	933	946
49	τ HCCN(16), τ HCCC(14), τ HCCC(25)	935	954
50	τ HCCN(14;10), τ HCCC(13)	951	969
51	τ CCCC(11), τ HCCC(17), τ HCCC(57)	976	981
52	τ CCCC(13), τ HCCC(25), τ HCCC(18;11;24)	982	1002
53	τ CCCC(18;27), τ HCCC(10), τ HCCC(55), τ HCCC(49)	1004	1010
54	v CC(19;17), v CC(15;13), δ CCC(29;26), δ CCC(26;21)	1019	1020
55	δ NNC(34), δ CCC(10)	1027	1045
56	v CC(18;13), δ HCC(16), δ CCC(10)	1052	1064
57	v CC(37), δ HCC(13), δ CCC(10)	1053	1085
58	v NN(61)	1084	1092
59	v CC(43), δ HCC(10)	1105	1115
60	v CC(28), δ HCC(13,12)	1106	1121
61	δ HCC(20,19)	1174	1199
62	v CC(14), δ HCC(66), δ HCC(67)	1183	1208
63	v CC(19), δ HCC(39), δ HCH(18)	1205	1251
64	v CC(24), δ HCC(36;13)	1208	1269
65	τ HCCN(13), δ HCC(20,22)	1210	1290
66	τ HCCN(10)	1219	1294
67	v CC(11), v CC(10)	1222	1298
68	v NC(21;17), δ OCN(13), δ CNN(10)	1231	1302
69	τ HCCN(12)	1250	1308
70	τ HCCN(10;11), δ OCN(13)	1285	1323
71	v CC(52), v CC(23)	1339	1335
72	v CC(69), δ HCC(12)	1340	1349
73	τ HCCN(24), δ HCC(14)	1355	1359
74	δ HCC(54), δ HCH(24)	1361	1367
75	δ HCC(51;25)	1367	1413
76	τ HCCN(22), v NN(12)	1371	1457
77	δ HNN(66)	1401	1471
78	v NC(21), v NN(23), δ HNC(15)	1450	1476
79	δ HNC(35), δ HNC(27)	1470	1513
80	δ HNC(19), δ HCH(58)	1474	1521
81	δ HCC(81)	1476	1538
82	v CC(24), δ HCC(12), δ HCC(27,11)	1487	1553
83	v CC(14), δ HCC(21), δ HCC(12;10)	1488	1557
84	v CC(11), δ HCC(28;16), δ HCC(31,13), δ CCC(11)	1532	1591

Table continuation

Seq.	Vibration Types	DFT	HF
85	v CC(12), v CC(27), v CC(20), δ CCC(12)	1629	1633
86	v CC(28;15,14), δ CCC(13)	1631	1656
87	v NC(52), v CC(12)	1645	1681
88	v CC(48), δ HCC(12)	1649	1761
89	v NC(13), v CC(38)	1652	1772
90	v OC(59;26)	1805	1980
91	v OC(55;21)	1833	2002
92	v CH(51;47)	3030	3158
93	v CH(41;37;11;10)	3042	3165
94	v CH(50;48)	3058	3195
95	v CH(39;11)	3111	3199
96	v CH(93), v CH(69), v CH(29)	3158	3220
97	v CH(38;11), v CH(11), v CH(39)	3160	3225
98	v CH(62;10;28)	3163	3242
99	v CH(31;30;17), v CH(19)	3170	3244
100	v CH(43;16;38)	3171	3310
101	v CH(54;16;23)	3179	3312
102	v CH(64;24)	3180	3320
103	v CH(86)	3189	3329
104	v CH(85)	3191	3340
105	v NH(50)	3537	3799
106	v NH(50)	3681	3928

Note: v: stretching vibration, δ: bending vibration, γ: out-of plane bending vibration, τ: torsion vibration

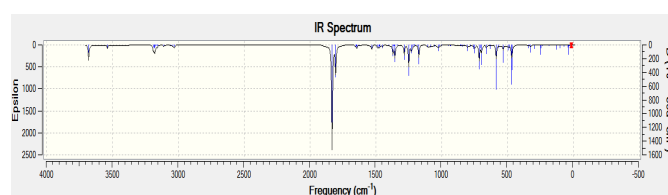


Figure 13 – Theoretical IR spectrums according to DFT/B3LYP/6-311G (d,p) level for molecule 3

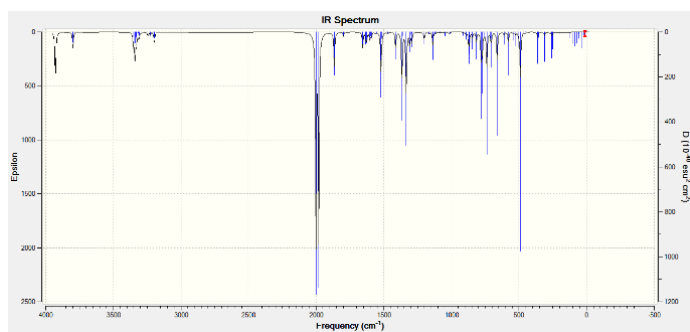


Figure 14 – Theoretical IR spectrums according to HF/B3LYP/6-311G (d,p) level for molecule 3

Table 8 – Vibration types and IR frequencies (cm^{-1}) of molecule 4

Seq.	Vibration Types	DFT	HF
1	τ CNNC(13), τ CCCN(36;34)	11	8
2	τ CCCC(21), τ CCCC(21;18)	20	11
3	τ CNNC(24;15), τ CCCN(18;12)	27	16
4	τ CNNC(18), τ NNCC(10), τ CCCN(30)	33	21
5	τ HCCC(60), τ CCCN(11)	37	36
6	δ CCN(10), τ CNNC(20), τ NNCC(22)	39	49
7	τ CNNC(11;12), τ CCCN(23)	40	57
8	δ CCC(11), τ CCCC(19), τ NNCC(15)	59	70
9	δ NNC(11), τ CCNN(56)	78	80
10	τ NNCC(16), γ CCCC(15), γ CCCC(16)	101	104
11	τ CNNC(11), τ NNCC(42), γ NCNC(17)	126	128
12	δ CCN(22), τ CCCC(13)	148	161
13	δ CCN(23)	192	209
14	τ CCCC(17), τ CCCC(10)	248	253
15	δ CCN(33), δ CCC(11)	249	275
16	δ CCC(13), τ CNNC(11)	279	296
17	τ CNNC(13), τ NNCC(22)	298	319
18	δ CNN(10), τ CCCC(11)	312	341
19	δ CNN(21)	331	365
20	δ CCC(16;13)	342	368
21	δ CCC(12;10), δ CCC(13;12)	379	407
22	τ HCCC(13), τ HCCC(19), τ CCCC(61;28), τ CCCC(57;12)	416	425
23	ν NC(12), ν NN(15), δ OCN(10)	425	455
24	τ HNNC(30)	466	462
25	τ HNNC(43)	470	490
26	τ CCCC(13), γ CCCC(19)	489	530
27	γ CCCC(21;15)	502	543
28	δ CCC(11), γ CCCC(10)	523	564
29	τ HNNC(14), γ ONNC(15;11)	534	579
30	δ CCC(22), τ HNNC(15)	583	653
31	δ OCN(27)	619	679
32	δ CCC(49), δ CCC(23;15)	636	699
33	δ CCC(18;17), γ NCNC(18)	654	713
34	δ CCC(13), γ NCNC(26)	664	736
35	τ HCCC(28), τ HCCC(10), τ CCCC(36;11)	717	758
36	ν CC(15)	739	772
37	ν CC(11), τ HCCC(43)	751	792
38	γ ONNC(40)	757	815
39	ν CC(10), τ HCCC(32)	767	830
40	δ CNN(21), δ NNC(17)	800	865
41	ν CC(17), τ HCCC(17)	829	869
42	ν CC(18), τ HCCC(16)	840	901

Table continuation

Seq.	Vibration Types	DFT	HF
42	τ HCCC(98)	846	921
43	ν CC(10)	854	929
44	τ HCCC(60), τ HCCC(16)	860	941
45	ν CC(13), τ HCCC(13)	863	946
46	ν NC(14)	909	1001
47	ν CC(10), δ HCC(15), δ HCC(12), τ HCCN(21;11)	929	1009
48	τ HCCC(27;14), τ HCCN(13)	935	1022
49	τ HCCC(15), τ HCCN(12;10)	951	1046
50	τ HCCC(70)	963	1069
51	τ HCCC(82)	970	1085
52	τ HCCC(21;19;10), τ HCCC(22), τ CCCC(18)	983	1092
53	τ HCCC(50), τ HCCC(14), τ CCCC(17)	1005	1115
54	ν CC(11), δ HCH(18), τ HCCC(44)	1010	1121
55	ν CC(32), δ CCC(10)	1019	1137
56	δ CNN(11;10), δ NNC(33)	1027	1161
57	δ HCH(13), δ CCC(30;29)	1040	1169
58	ν CC(23;13), δ HCC(18), δ CCC(10)	1053	1178
59	δ HCH(15), τ HCCC(52;12)	1063	1199
60	ν NN(61)	1084	1208
61	ν CC(25), ν CC(17), δ HCC(14;11)	1106	1251
62	ν CC(12), ν CC(22), δ HCH(53)	1140	1269
63	δ HCC(15), δ HCC(16)	1175	1290
64	ν CC(12), δ HCC(65)	1183	1294
65	ν CC(11), δ HCC(13), δ HCC(20), τ HCCN(13;11)	1208	1298
66	ν CC(17), δ HCC(30), δ HCH(70)	1209	1302
67	ν CC(37), ν CC(37), ν CC(17;13)	1222	1308
68	ν NC(14;20), δ OCN(11)	1231	1323
69	ν CC(16;10), δ CCC(13), δ HCH(19)	1234	1335
70	δ HCC(12), δ HCC(11)	1251	1349
71	δ NCN(12), δ CNN(11), τ HCCN(11)	1286	1359
72	ν CC(37), ν CC(25), δ HCH(13)	1332	1367
73	ν CC(27;11), ν CC(16), δ HCC(10)	1339	1413
74	ν CC(12), δ HCH(70)	1349	1457
75	τ HCCN(15;38)	1356	1471
76	δ HCC(48), δ HCC(23)	1368	1476
77	ν NN(10), τ HCCN(32)	1371	1513
78	δ HNN(66)	1400	1521
79	δ HCH(89)	1416	1538
80	ν CC(18), δ HCH(39)	1444	1553
81	ν NC(20), ν NN(23), δ HNC(13)	1449	1557
82	δ HNC(41), δ HCH(24)	1470	1591
83	δ HNC(11), δ HCH(62)	1473	1597
84	δ HNC(10), δ HCC(77)	1476	1604

Table continuation

Seq.	Vibration Types	DFT	HF
85	ν CC(12), δ HCC(22), δ HCC(12;10)	1488	1608
86	δ HCH(70), τ HCCC(16)	1491	1612
87	δ HCH(65), τ HCCC(14)	1497	1625
88	δ HCC(31), δ HCC(18), δ CCC(10)	1532	1633
89	δ HCH(59)	1551	1656
90	ν CC(12), ν CC(22;21), δ CCC(11)	1619	1681
91	ν CC(12), ν CC(40), δ CCC(12)	1629	1761
92	ν NC(64)	1647	1772
93	ν CC(20;16;12), δ HCC(11)	1649	1798
94	ν CC(55), δ HCH(18)	1661	1812
95	ν OC(59;26)	1805	1980
96	ν OC(55;21)	1832	2001
97	ν CH(97)	3023	3158
98	ν CH(50;47)	3028	3165
99	ν CH(38;11;10), ν CH(41)	3043	3195
100	ν CH(48;49)	3056	3199
101	ν CH(90)	3076	3220
102	ν CH(89)	3103	3225
103	ν CH(10)	3110	3242
104	ν CH(39;11)	3111	3244
105	ν CH(77;23)	3153	3310
106	ν CH(93)	3158	3312
107	ν CH(62), ν CH(29)	3164	3320
108	ν CH(99)	3169	3329
109	ν CH(41;18), ν CH(39)	3171	3330
110	ν CH(99)	3172	3333
111	ν CH(54;17), ν CH(20)	3179	3340
112	ν CH(86)	3189	3351
113	ν NH(50)	3539	3799
114	ν NH(50)	3681	3928

Note: ν : stretching vibration, δ : bending vibration, γ : out-of plane bending vibration, τ : torsion vibration

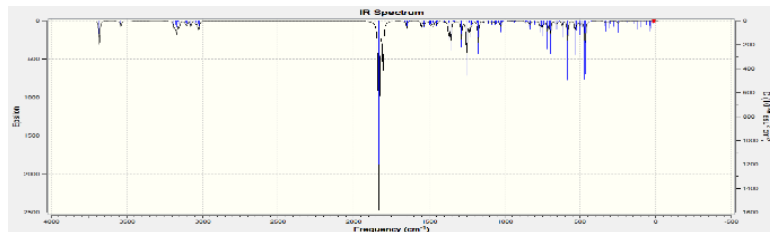


Figure 15 – Theoretical IR spectra according to DFT/B3LYP/6-311G (d,p) level for molecule 4.

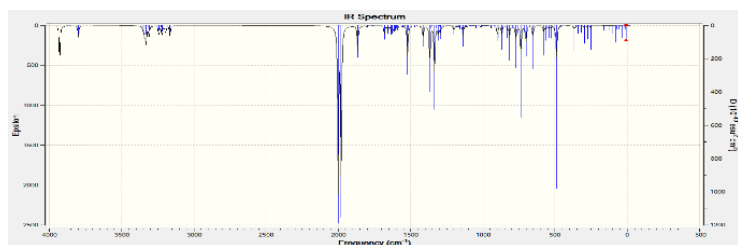


Figure 16 – Theoretical IR spectrums according to HF/B3LYP/6-311G (d,p) level for molecule 4.

Table 9 – Vibration types and IR frequencies (cm^{-1}) of molecule 5

1	τ NCCC(47), γ NCCN(17), τ CCCN(20)	10	10
2	τ NCCC(18), τ CCCN(34), τ CCCC(30)	18	15
3	τ CCCN(11;30), τ CCCC(33)	24	19
4	τ NCCC(16), τ CCCN(40), τ CCCC(19)	30	34
5	δ CCC(14), δ NCC(12), δ CCC(10), τ CCCC(16), γ CCCC(31)	38	43
6	δ CNN(14), γ NCCN(34)	39	56
7	τ CNNC(37;15)	54	69
8	δ NNC(11), τ CCNN(52)	78	78
9	δ CCC(12), τ CCCC(11), γ NCCN(13)	100	104
10	γ NCNC(17), τ NNCC(32), τ CNNC(32)	125	127
11	δ NCC(17), δ CCC(12), τ CCCC(32), γ CICCC(18)	135	148
12	δ NCC(22)	182	199
13	δ CICN(31), γ NCCN(14)	243	251
14	δ CCC(12), δ CICC(43)	248	268
15	δ CCC(10), τ CCCC(35;13)	254	276
16	τ NNCC(33), τ CNNC(10)	297	315
17	γ CCCC(16), γ CICCC(29), τ CCCC(16)	307	336
18	δ CCC(49)	328	355
19	δ CCC(19), δ OCN(10), δ NNC(24)	341	365
20	δ CCC(22;20), δ CICC(30)	366	396
21	ν CIC(22), δ CCC(12)	401	435
22	τ HCCC(16), τ CCCC(16;15)	415	452
23	τ HCCC(17), τ CCCC(79)	418	456
24	τ HNNC(12)	446	483
25	τ HNNC(31;14)	466	493
26	δ OCN(16)	472	503
27	τ CCCC(29;18;10)	495	536
28	τ CCCC(21;22), γ CCCC(15), γ CICCC(22)	508	557
29	δ CCC(13), τ HNNC(11), γ ONNC(13;11)	534	579
30	δ OCN(36)	582	647
31	δ CCC(51;18;15)	608	679
32	δ CCC(28;18;14)	636	694
33	γ NCNC(26)	647	712
34	ν CIC(13)	674	724

Table continuation

35	τ HNNC(12)	694	743
36	τ HCCC(10), τ CCCC(36)	701	756
37	τ HCCC(13), τ HCCC(12), τ CCCC(23;15)	717	772
38	τ HCCC(17)	748	813
39	τ HCCC(10), τ CCCC(11)	757	826
40	δ CNN(13;15)	759	863
41	γ ONNC(41;39), τ CNNC(10)	796	869
42	ν CC(16)	828	891
42	ν CC(14)	831	899
43	δ CCC(11)	834	921
44	τ HCCC(99)	859	934
45	τ HCCC(58), τ HCCC(27)	864	946
46	τ HCCC(47), γ CCCC(12)	909	953
47	ν NC(13), δ CCN(12)	933	1002
48	δ HCC(15), δ HCC(16), τ HCCC(16), τ HCCN(12)	935	1016
49	τ HCCC(16;10), τ HCCN(21)	951	1022
50	τ HCCC(46;11), τ HCCC(18)	964	1045
51	τ HCCC(71), τ CCCC(10)	972	1076
52	ν CC(42), δ CCC(53)	983	1085
53	τ HCCC(42;11), τ HCCC(84), τ CCCC(16;14)	1006	1095
54	δ CCC(12), δ CCC(59), δ HCC(10)	1019	1106
55	τ HCCC(34;16), τ CCCC(21)	1026	1115
56	ν CC(32), δ CCC(13;11), δ HCC(15)	1033	1121
57	δ CNN(11), δ NNC(40)	1053	1137
58	ν CC(28), δ HCC(19)	1086	1169
59	ν CC(29), δ HCC(21)	1102	1172
60	ν CC(11), ν CC(35), ν CIC(22), δ HCC(13)	1106	1195
61	ν CC(19), ν CC(27;10), δ HCC(14)	1132	1204
62	δ HNN(12)	1173	1247
63	ν CC(26), δ HCC(28)	1183	1290
64	ν CC(25), δ HCC(34), δ HCC(13)	1204	1292
65	ν CC(10), δ HCC(67)	1208	1294
66	ν CC(12), ν NN(61), δ HCC(13), δ HCC(22;16)	1209	1308
67	δ HCC(12;11), τ HCCN(12)	1222	1310
68	ν CC(12), ν CC(11), δ HCC(15)	1230	1333
69	ν NC(20), ν CC(10)	1250	1343
70	δ HCC(20), δ HCC(10;26), τ HCCC(10)	1287	1358
71	ν CC(12), δ HCC(16), δ HCC(10)	1321	1362
72	ν NC(28)	1339	1365
73	ν NC(11)	1341	1414
74	ν NC(13), δ CNN(17), δ NNC(10), τ HCCN(14)	1355	1445
75	δ HCC(85)	1367	1471
76	δ HCC(16), δ HCC(20;17;24)	1401	1513
77	ν NC(11), ν CC(12), τ HCCN(29)	1439	1521

Table continuation

78	v CC(15), τ HCCN(33)	1450	1552
79	v CC(11), v CC(14), δ HCC(39)	1470	1554
80	δ HNN(60)	1474	1590
81	δ HCC(42;32), τ HCCN(11)	1476	1598
82	δ HCC(50;42)	1488	1604
83	v CC(14), δ HCC(42)	1526	1627
84	v NC(13), δ HNC(48)	1532	1632
85	v NC(32;18), δ HNC(20)	1619	1656
86	δ CCC(11), δ HCC(33), δ HCC(13)	1629	1660
87	v CC(16), δ CCC(10), δ HCC(55)	1641	1762
88	v CC(51), δ CCC(14;10)	1648	1795
89	v CC(37;27), v CC(12;22), δ CCC(11), δ HCC(10)	1649	1798
90	v CC(12), v CC(29), δ HCC(20)	1807	1866
91	v CC(48), δ HCC(12)	1834	1983
92	v NC(69)	3031	2003
93	v OC(59;15)	3042	3197
94	v OC(65;19)	3058	3198
95	v CH(68), v CH(31)	3059	3229
96	v CH(29), v CH(66)	3111	3243
97	v CH(53), v CH(46)	3158	3309
98	v CH(44), v CH(51)	3164	3320
99	v CH(20), v CH(69)	3169	3328
100	v CH(74), v CH(13)	3170	3329
101	v CH(24;49), v CH(19)	3171	3331
102	v CH(52;23), v CH(16)	3179	3341
103	v CH(85), v CH(11)	3189	3351
104	v CH(89)	3203	3365
105	v CH(93)	3204	3366
106	v CH(28), v CH(72)	3371	3430
107	v CH(24), v CH(75)	3372	3433
108	v NH(50)	3536	3797
109	v NH(50)	3679	3926

Note: v: stretching vibration, δ: bending vibration, γ: out-of plane bending vibration, τ: torsion vibration

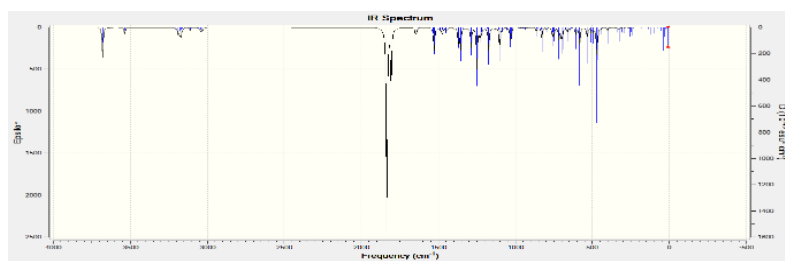


Figure 17 – Theoretical IR spectra according to DFT/B3LYP/6-311G (d,p) level for molecule 5

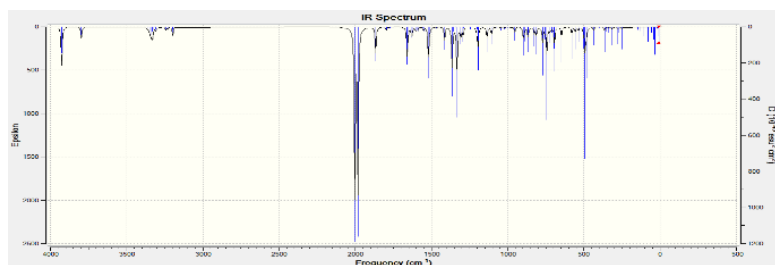


Figure 18 – Theoretical IR spectra according to HF/B3LYP/6-311G (d,p) level for molecule 5

To examine how molecules interact with ultraviolet light, scientists employ a technique called UV (ultraviolet) spectral analysis in analytical chemistry and other disciplines. Since ultraviolet light has shorter wavelengths and more energy than visible light, it can excite molecular electrons to states with higher energies. This interaction between UV light and molecules can reveal important details about the composition, characteristics, and chemical structure of the substances being examined. UV spectral analysis includes shining UV light through a sample and observing how much of it is absorbed

or transmitted at various wavelengths. The UV absorption spectra that results can shed light on the electronic transitions occurring inside the molecules in the sample. Compounds may be identified, their concentrations can be measured, and numerous chemical processes and interactions can be researched using this data. When the theoretical UV-visible spectrum of the molecules drawn according to the DFT and HF methods and given in Figure 19-23 are examined, it has been observed that the spectra drawn according to both methods are generally compatible with each other.

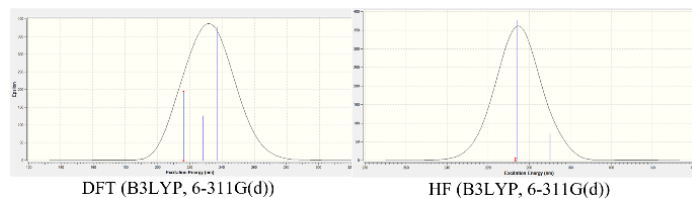


Figure 19 – Theoretical UV-visible spectrum for studied molecule 1

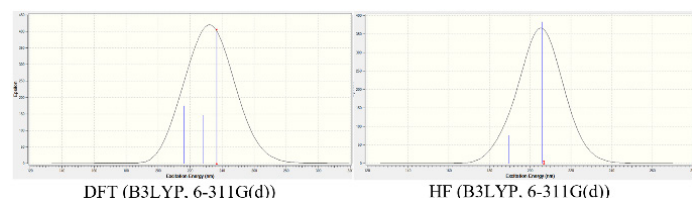


Figure 20 – Theoretical UV-visible spectrum for studied molecule 2

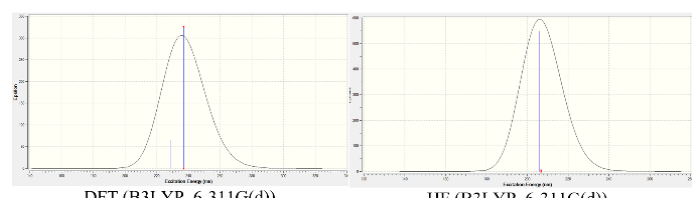


Figure 21 – Theoretical UV-visible spectrum for studied molecule 3

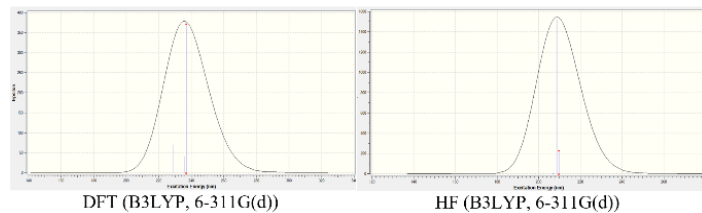


Figure 22 – Theoretical UV-visible spectrum for studied molecule 4

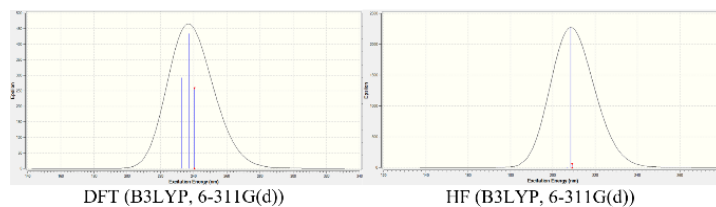


Figure 23 – Theoretical UV-visible spectrum for studied molecule 5

In computational chemistry, the idea of molecular electrostatic potential (MEP) is used to examine and depict molecules' electrostatic characteristics. It offers information about how electric charges are distributed within molecules, which in turn affects a number of molecular interactions, characteristics, and forces, including bonding and reactivity. The partial atomic charges that are given to the atoms in a molecule are the source of MEP and are frequently computed using quantum mechanical techniques like density functional theory (DFT) or Hartree-Fock computations. The distribution of electron density surrounding each atom is represented by these partial charges, which also contribute to the

molecule's overall electrostatic potential. Typically, color maps or contour plots are used to show the MEP graphically. In these figures, the blue patches with positive MEP often denote electron-poor regions, which are places with an electron-deficient environment. In contrast, areas with negative MEP are frequently depicted in red to denote electron-rich zones. Neutral areas are usually shown in white. When the Molecular Electrostatic Potential (MEP) shapes we obtained in this framework and given in Figure 24-28 are examined, it is seen that electron-poor regions, electron-rich regions and neutral regions of each molecule are clearly distinct.

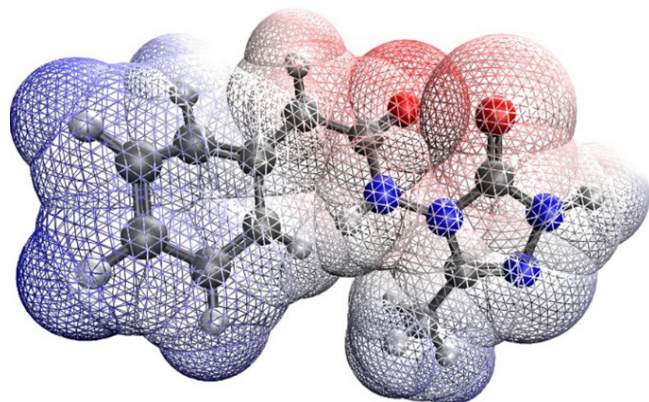


Figure 24 – Molecular electrostatic potential (MEP) for molecule 1

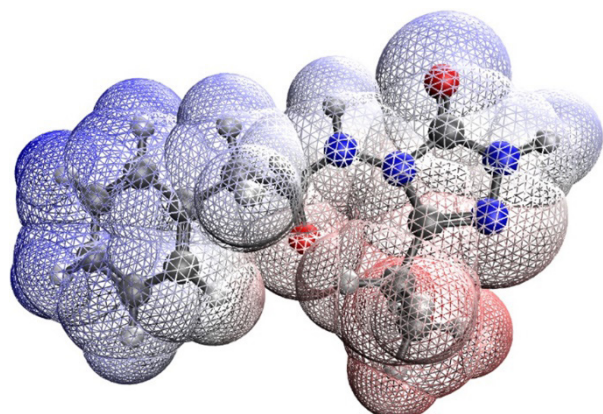


Figure 25 – Molecular electrostatic potential (MEP) for molecule 2

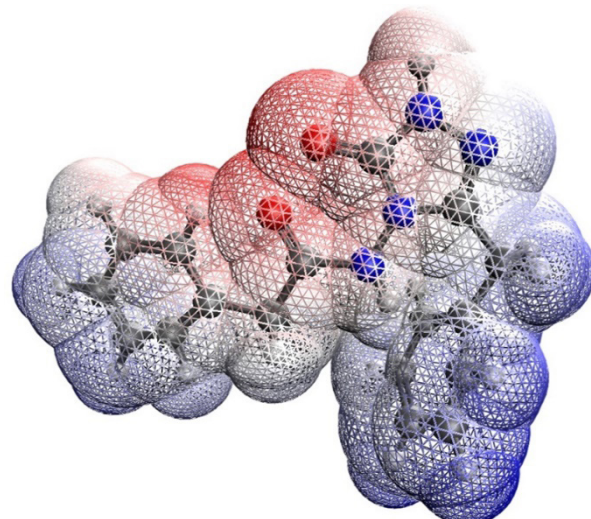


Figure 26 – Molecular electrostatic potential (MEP) for molecule 3

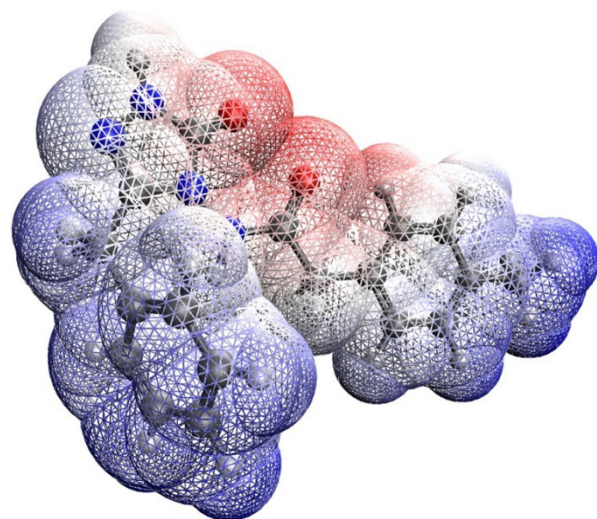


Figure 27 – Molecular electrostatic potential (MEP) for molecule 4

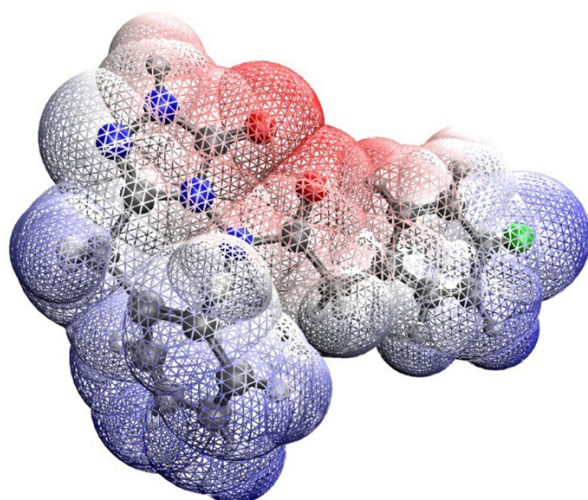


Figure 28 – Molecular electrostatic potential (MEP) for molecule 5

Conclusion

By conducting theoretical studies of these five molecules, which we had previously synthesized, we showed that they could be evaluated especially in drug development. It is especially important that the Density Functional Theory, (DFT, B3LYP) / Hartree Fock, (HF, B3LYP) methods we used in this theoretical study are widely used in the literature. Properties such as FT-IR and UV-vis spectral values, bond angles, bond lengths, dipole moments, highest occupied molecular orbital (HOMO), lowest unoccupied molecular orbital (LUMO) energy and total energy, mulliken charges and molecular electrostatic potential (MEP). Determination is important so that these molecules can be used for purposes other than being used as drug active ingredients.

References

1. Cao, X.; Wang, W.; Wang, Sh. and Bao, L. Asymmetric synthesis of novel triazole derivatives and their in vitro antiviral activity and mechanism of action. *Eur. J. Med. Chem.* 2017, 139, 718-725.
2. Gao, F.; Wang, T.; Xiao, J. and Huang, G. Antibacterial activity study of 1, 2, 4-triazole derivatives. *Eur. J. Med. Chem.* 2019, 173, 274-281.
3. Sadeghpour, H.; Khabnadideh, S.; Zomorodian, K.; Pakshir, K.; Hoseinpour, K.; Javid, N.; Faghih-Mirzaei, E. and Rezaei, Z. Design, synthesis, and biological activity of new triazole and nitro-triazole derivatives as antifungal agents. *Molecules* 2017, 22, 1150-1161.
4. Cheng, Y.N.; Jiang, Zh.H.; Sun, L.Sh.; Su, Z.Y.; Zhang, M.M. and Li, H.L. Synthesis of 1,2,4-triazole benzoyl arylamine derivatives and their high antifungal activities. *Eur. J. Med. Chem.* 2020, 200, 112463-112474.
5. Tsukuda, T.; Shiratori, Y.; Watanabe, M.; Onsuka, H.; Hattori, K.; Shirai, M. and Shimma, N. Modeling, synthesis and biological activity of novel antifungal agents-I. *Bioorg. Med. Chem. Lett.* 1998, 8, 1819-1829.
6. Arndt, C.A.S.; Walsh, T.J.; Pizzo, F.M. and Poplack, D.G. Cerebrospinal fluid penetration of fluconazole: implications for antifungal therapy in patients with acquired immunodeficiency syndrome. *J. Infect. Dis.* 1988, 157(1), 178-180.
7. Mbailey, E.; Krakovsky, D.J. and Rybak, M.J. The triazole antifungal agents: A review of itraconazole and fluconazole. *Pharmacotherapy* 1990, 10, 146-153.
8. Roberts, J.; Schock, K.; Marino, S. and Andriole, V.T. Efficacies of two new antifungal agents, the triazole rauconazole and the echinocandin LY-303366, in an experimental model of invasive aspergillosis. *Antimicrob. Agents Chemother.* 2000, 44(12), 3381-3388.
9. Espinel-Ingroff, A. In vitro activity of the new triazole voriconazole (UK-109, 496) against opportunistic filamentous and dimorphic fungi and common and emerging yeast pathogens. *J. Clin. Microbiol.* 1998, 36, 198-202.
10. Sabo, J.A. and Abdel-Rahman, S.M. Voriconazole: a new triazole antifungal. *Ann. Pharmacother.* 2000, 34(9), 1032-1043.

11. Johnson, L.B. and Kauffman, C.A. Voriconazole: a new triazole antifungal agent. *Clin. Infect. Dis.* 2003, 36(5), 630-637.
12. Pfaller, M.A.; Messer, S. and Jones, R.N. Activity of a new triazole, Sch 56592, compared with those of four other antifungal agents tested against clinical isolates of candida spp. and saccharomyces cerevisiae. *Antimicrob. Agents. Chemother.* 1997, 41(2), 233-235.
13. Neenu, G.; Arun K, S.; Manisha, S.; Venkaraddi Mangannavar, C. and Gurubasavaraj Veeranna, P. Antitubercular potential of novel isoxazole encompassed 1, 2, 4-triazoles: design, synthesis, molecular docking study and evaluation of antitubercular activity. *Anti-Infect. Agents* 2021, 19(2), 147-161.
14. Mohan Krishna, K.; Inturi, B.; Pujar, G.V.; Purohit, M.N. and Vijaykumar, G.S. Design, synthesis and 3D-QSAR studies of new diphenylamine containing 1, 2, 4-triazoles as potential antitubercular agents. *Eur. J. Med. Chem.* 2014, 84, 516-529.
15. Keri, R.S.; Patil, S.A.; Budagumpi, S. and Nagaraja, B.M. Triazole: a promising antitubercular agent. *Chem. Biol. Drug. Des.* 2015, 86(4), 410-423.
16. Chinthakindi, P.K.; Sangwan, P.L.; Farooq, S.; Aleti, R.R.; Kaul, A.; Saxena, A.K.; Murthy, Y.L.N.; Vishwakarma, R.A. and Koul, S. Diminutive effect on T and B-cell proliferation of non-cytotoxic α -santonin derived 1, 2, 3-triazoles: A report. *Eur. J. Med. Chem.* 2013, 60, 365-375.
17. Liu, J.; Liu, Q.; Yang, X.; Xu, Sh.; Zhang, H.; Bai, R.; Yao, H.; Jiang, J.; Shen, M.; Wu, X. and Xu, J. Design, synthesis, and biological evaluation of 1, 2, 4-triazole bearing 5-substituted biphenyl-2-sulfonamide derivatives as potential antihypertensive candidates. *Bioorg. Med. Chem.* 2013, 21(24), 7742-7751.
18. Abuo-Rahma, G.E.-D.A.; Abdel-Aziz, M.; Farag, N.A. and Kaoud, T.S. Novel 1-[4-(Aminosulfonyl) phenyl]-1H-1, 2, 4-triazole derivatives with remarkable selective COX-2 inhibition: Design, synthesis, molecular docking, anti-inflammatory and ulcerogenicity studies. *Eur. J. Med. Chem.* 2014, 83, 398-408.
19. Abdel-Aziz, M.; Beshr, E.A.; Abdel-Rahman, I.M.; Ozadali, K.; Tan, O.U. and Aly, O.M. 1-(4-Methoxyphenyl)-5-(3, 4, 5-trimethoxy phenyl)-1H-1,2,4-triazole-3-carboxamides: Synthesis, molecular modeling, evaluation of their anti-inflammatory activity and ulcerogenicity. *Eur. J. Med. Chem.* 2014, 77, 155-165.
20. Huang, L.; Ding, J.; Li, M.; Hou, Z.; Geng, Y.; Li, X. and Yu, H. Discovery of [1, 2, 4]-triazolo [1, 5-a] pyrimidine-7 (4H)-one derivatives as positive modulators of GABAA1 receptor with potent anticonvulsant activity and low toxicity. *Eur. J. Med. Chem.* 2020, 185, 111824-111833.
21. Plech, T.; Luszczki, J.J.; Wujec, M.; Flieger, J. and Pizon, M. Synthesis, characterization and preliminary anticonvulsant evaluation of some 4-alkyl-1, 2, 4-triazoles. *Eur. J. Med. Chem.* 2013, 60, 208-215.
22. Vijesh, A.M.; Isloor, A.M.; Shetty, P.; Sundarshan, S. and Fun, H.K. New pyrazole derivatives containing 1, 2, 4-triazoles and benzoxazoles as potent antimicrobial and analgesic agents. *Eur. J. Med. Chem.* 2013, 62, 410-415.
23. Kholodnyak, S.V.; Schabelnyk, K.P.; Zhernova, G.O.; Sergeieva, T.Yu.; Ivchuk, V.V.; Voskoboynik, O.Yu.; Kovalenko, S.I.; Trzhetsinskii, S.D.; Okovytyy, S.I. and Shishkina, S.V. Hydrolytic cleavage of the pyrimidine ring in 2-aryl-[1, 2, 4] triazole [1, 5-c] quinazolines: physico-chemical properties and the hypoglycemic activity of the compounds synthesized. *News of Pharmacy* 2015, 83(3), 9-17.
24. Chelamalla, R.; Akena, V. and Manda, S. Synthesis of N-arylidene-2-(5-aryl-1H-1, 2, 4-triazol-3-ylthio) acetohydrazides as antidepressants. *Med. Chem. Res.* 2017, 26, 1359-1366.
25. Radhika, C.; Venkatesham, A. and Sarangapani, M. Synthesis and antidepressant activity of di substituted-5-aryl-1,2,4-triazoles. *Med. Chem. Res.* 2012, 21, 3509-3513.
26. El-Sherief, H.A.; Youssif, B.G.M.; Bukhari, S.N.A.; Abdelazeem, A.H.; Abdel-Aziz, M. and Abdel-Rahman, H.M. Synthesis, anticancer activity and molecular modeling studies of 1, 2, 4-triazole derivatives as EGFR inhibitors. *Eur. J. Med. Chem.* 2018, 156, 774-789.
27. El-Sherief, H.A.M.; Youssif, B.G.M.; Bukhari, S.N.A.; Abdel-Aziz, M. and Abdel-Rahman, H.M. Novel 1, 2, 4-triazole derivatives as potential anticancer agents: Design, synthesis, molecular docking and mechanistic studies. *Bioorg. Chem.* 2018, 76, 314-325.
28. Turky, A.; Bayoumi, A.H.; Sherbiny, F.F.; El-Adl, K. and Abulkhair, H.S. Unravelling the anticancer potency of 1, 2, 4-triazole-N-arylamide hybrids through inhibition of STAT3: synthesis and in silico mechanistic studies. *Mol. Divers.* 2021, 25(1), 403-420.
29. Xu, K.; Huang, L.; Xu, Zh.; Wang, Y.; Bai, G.; Wu, Q.; Wang, X.; Yu, Sh. and Jiang, Y. Design, synthesis, and antifungal activities of novel triazole derivatives containing the benzyl group. *Drug Des. Devel. Ther.* 2015, 9, 1459-1467.

30. Chaia, B.; Qian, X.; Cao, S.; Liu, H. and Song, G. Synthesis and insecticidal activity of 1,2,4-triazole derivatives. *Arkivoc* 2003, ii, 141-145.
31. Naito, Y.; Akahoshi, F.; Takeda, S.; Okada, T.; Kajii, M.; Nishimura, H.; Sugiura, M.; Fukaya, C. and Kagitani, Y. Synthesis and pharmacological activity of triazole derivatives inhibiting eosinophilia. *J. Med. Chem.* 1996, 39(15), 3019-3029.
32. Oruc, E.E.; Rollas, S.; Kabasakal, L. and Uysal, M.K. The in vivo metabolism of 5-(4-nitrophenyl)-4-phenyl-2,4-dihydro-3H-1,2,4-triazole-3-thione in rats. *Drug. Metabol. Drug. Interact.* 1999, 15(2-3), 127-140.
33. Maddila, S.; Pagadala, R. and Jonnalagadda, S.B. Synthesis and insecticidal activity of tetrazole linked triazole derivatives. *J. Het. Chem.* 2014, 52(2), 487-491.
34. Oh, K.; Yamada, K.; Asami, T. and Yoshizawa, Y. Synthesis of novel brassinosteroid biosynthesis inhibitors based on the ketoconazole scaffold. *Bioorg. Med. Chem. Lett.* 2012, 22(4), 1625-1628.
35. Santen, J.R. Inhibition of aromatase: insights from recent studies. *Steroids* 2003, 68(7-8), 559-567.
36. Clemons, M.; Coleman, R.E. and Verma, S. Aromatase inhibitors in the adjuvant setting: bringing the gold to a standard? *Cancer Treat. Rev.* 2004, 30, 325-332.
37. Delea, E.; El-Ouagari, K.; Karnon, J. and Sofrygin, O. Cost-effectiveness of letrozole versus tamoxifen as initial adjuvant therapy in postmenopausal women with hormone-receptor positive early breast cancer from a Canadian perspective. *Breast Cancer Res. Treat.* 2008, 108(3), 375-387.
38. Christova, K.; Shilkaitis, A.; Green, A.; Mehta, R.G.; Grubbs, C.; Kelloff, G. and Lubet, R. Cellular responses of mammary carcinomas to aromatase inhibitors: Effects of vorozole. *Breast Cancer Res. Treat.* 2000, 60, 117-128.
39. Roman, G.; Rahman, M.N.; Vukomanovic, D.; Jia, Z.; Nakatsu, K. and Szarek, W.A. Heme oxygenase inhibition by 2-oxy-substituted 1-azolyl-4-phenyl butanes: effect of variation of the azole moiety. X-ray crystal structure of human heme oxygenase-1 in complex with 4-phenyl-1-(1H-1,2,4-triazol-1-yl) -2-butanone. *Chem. Biol. Drug. Des.* 2010, 75(1), 68-90.
40. Pagacz-Kostrzewska, M.; Bronisz, R. and Wierzejewska, M. Theoretical and matrix isolation FTIR studies of 3-amino-1,2,4-triazole and its isomers. *Chem. Phys. Lett.* 2009, 473(4-6), 238-246.
41. Al-Tamimi, A.S. Electronic structure, hydrogen bonding and spectroscopic profile of a new 1,2,4-triazole-5(4H)-thione derivative: A combined experimental and theoretical (DFT) analysis. *J. Mol. Str.* 2016, 1120, 215-227.
42. Ayeni, A.O.; Watkins G.M. and Hosten, E.C. Polymorphism of a new Mannich base-[4-methyl-2-((4-(4-nitrophenyl)piperazin-1-yl)methyl) phenol]. *J. Mol. Str.* 2018, 1160, 38-45.
43. Raj, A.D.; Jeeva, M.; Shankar, M.; Prabhu, G.V.; Vimalan, M.; Potheher, I.V. Synthesis, growth, physicochemical properties and DFT calculations of 2-naphthol substituted Mannich base 1-(morpholino (phenyl) methyl) naphthalen-2-ol: A non linear optical single crystal. *J. Mol. Str.* 2017, 1147, 763-775.
44. Boobalan, M.S.; Amaladasan, M.; Ramalingam, S.; Tamilvendan, D.; Prabhu, G.V. and Bououdina, M. First principles and DFT supported investigations on vibrational spectra and electronic structure of 2-((phenyl amino)methyl)isoindoline-1,3-dione-An antioxidant active Mannich base. *Spectrochim. Acta A Mol. Biomol. Spectrosc.* 2015, 137, 962-978.
45. Fu, A.; Li, H.; Si, H.; Yuan, S. and Duan, Y. Theoretical studies of stereoselectivities in the direct syn- and anti-Mannich reactions catalyzed by different amino acids. *Tetrahedron: Asymmetry* 2008, 19(19), 2285-2292.
46. Pajak, J.; Rospenk, M.; Maes, G. and Sobczyk, L. Matrix-isolation FT-IR and DFT theoretical studies of the intramolecular hydrogen bonding in Mannich bases. *Chem. Phys.* 2006, 320(2), 229-238.
47. Al-Wabli, R.I.; Govindarajan, M.; Almutairi, M.S. and Attia, M.I. Spectral characterization, computed frequencies analysis and electronic structure calculations on (1E)-N-hydroxy-3-(1H-imidazol- 1-yl)-1-phenylpropan-1-imine: An oxime-bearing precursor to potential antifungal agents. *J. Mol. Str.* 2018, 1168, 264-279.
48. Diez-Martinez, A.; Tejero, T. and Merino, P. Experimental and theoretical studies on Mannich-type reactions of chiral non-racemic N-(benzyloxyethyl) nitrones. *Tetrahedron: Asymmetry* 2010, 21(24), 2934-2943.
49. Abramov, Yu. A.; Volkov, A.V. and Coppens, P. On the evaluation of molecular dipole moments from multipole refinement of X-ray diffraction data. *Chem. Phys. Lett.* 1999, 311(1-2), 81-86.
50. Handy, N.C.; Maslen, P.E.; Amons, R.D.; Audrows, J.S.; Murroy, C.W. and Lawing, G. The harmonic frequencies of benzene. *Chem. Phys. Lett.* 1992, 197(4-5), 506-515.

51. Forsyth, D.A. and Sebag, A.B. Computed ¹³C NMR Chemical Shifts via Empirically Scaled GIAO Shieldings and Molecular Mechanics Geometries. Conformation and Configuration from ¹³C Shifts. *J. Am. Chem. Soc.* 1997, 119(40), 9483-9494.
52. Sebag, A.B.; Forsyth, D.A. and Plante, M.A. Conformation and configuration of tertiary amines via GIAO-derived (¹³C) NMR chemical shifts and a multiple independent variable regression analysis. *J. Org. Chem.* 2001, 66 (24), 7967-7973.
53. Turhan Irak, Z. and Gümüş, S. Heterotricyclic compounds via click reaction: A computational study. *Noble Int. J. Sci. Res.* 2017, 1(7), 80-89.
54. Beytur, M.; Turhan Irak, Z.; Manap, S. and Yüksel, H. Synthesis, characterization and theoretical determination of corrosion inhibitor activities of some new 4,5-dihydro-1H-1,2,4-triazol-5-one derivatives. *Heliyon* 2019, 5(6), 1-8.
55. Turhan Irak, Z. and Beytur, M. Theoretical study on the investigation of antioxidant properties of some 4-benzylidenamino-4,5-dihydro-1H-1,2,4-triazol-5-one derivatives. *Iğdır Univ. J. Inst. Sci. Tech.* 2019, 9(1), 512-521.
56. Ditchfield, R. Self-consistent perturbation theory of diamagnetism. *Mol. Phys.* 1974, 27(4), 789-807.
57. Wolinski, K.; Hinton, J.F. and Pulay, P. Efficient implementation of the gauge-independent atomic orbital method for NMR chemical shift calculations. *J. Am. Chem. Soc.* 1990, 112, 8251-8260.
58. Cheeseman, J.R.; Trucks, G.W.; Keith, T.A. and Frisch, M.J. A comparison of models for calculating nuclear magnetic resonance shielding tensors. *J. Chem. Phys.* 1996, 104(14), 5497-5509.
59. Friesner, R.A.; Murphy, R.B.; Beachy, M.D.; Ringnalda, M.N.; Pollard, W.T.; Dunietz, B.D. and Cao, Y. Correlated ab initio electronic structure calculations for large molecules. *J. Phys. Chem. A* 1999, 103(13), 1913-1928.
60. Alkan, M.; Yüksel, H.; İslamoğlu, F.; Bahçeci, Ş.; Calapoğlu, M.; Elmastaş, M.; Akşit, H. and Özdemir, M. A study on 4-acylamino-4,5-dihydro-1H-1,2,4-triazol-5-ones. *Molecules* 2007, 12, 1805-1816.